NIST SPECIAL PUBLICATION 400-100

U.S. DEPARTMENT OF COMMERCE/Technology Administration
National Institute of Standards and Technology

Semiconductor Measurement Technology:

Thin Film Reference Materials Development
Final Report for CRADA CN-1364

Barbara J. Belzer, Keith Eberhardt, Deane Chandler-Horowitz,
James R. Ehrstein, and Prabha Durgapal

The National Institute of Standards and Technology was established in 1988 by Congress to "assist industry in the development of technology . . . needed to improve product quality, to modernize manufacturing processes, to ensure product reliability . . . and to facilitate rapid commercialization . . . of products based on new scientific discoveries."

NIST, originally founded as the National Bureau of Standards in 1901, works to strengthen U.S. industry's competitiveness; advance science and engineering; and improve public health, safety, and the environment. One of the agency's basic functions is to develop, maintain, and retain custody of the national standards of measurement, and provide the means and methods for comparing standards used in science, engineering, manufacturing, commerce, industry, and education with the standards adopted or recognized by the Federal Government.

As an agency of the U.S. Commerce Department's Technology Administration, NIST conducts basic and applied research in the physical sciences and engineering, and develops measurement techniques, test methods, standards, and related services. The Institute does generic and precompetitive work on new and advanced technologies. NIST's research facilities are located at Gaithersburg, MD 20899, and at Boulder, CO 80303. Major technical operating units and their principal activities are listed below. For more information contact the Publications and Program Inquiries Desk, 301-975-3058.

Office of the Director
- National Quality Program
- International and Academic Affairs

Technology Services
- Standards Services
- Technology Partnerships
- Measurement Services
- Technology Innovation
- Information Services

Advanced Technology Program
- Economic Assessment
- Information Technology and Applications
- Chemical and Biomedical Technology
- Materials and Manufacturing Technology
- Electronics and Photonics Technology

Manufacturing Extension Partnership Program
- Regional Programs
- National Programs
- Program Development

Electronics and Electrical Engineering Laboratory
- Microelectronics
- Law Enforcement Standards
- Electricity
- Semiconductor Electronics
- Electromagnetic Fields[1]
- Electromagnetic Technology[1]
- Optoelectronics[1]

Chemical Science and Technology Laboratory
- Biotechnology
- Physical and Chemical Properties[2]
- Analytical Chemistry
- Process Measurements
- Surface and Microanalysis Science

Physics Laboratory
- Electron and Optical Physics
- Atomic Physics
- Optical Technology
- Ionizing Radiation
- Time and Frequency[1]
- Quantum Physics[1]

Materials Science and Engineering Laboratory
- Intelligent Processing of Materials
- Ceramics
- Materials Reliability[1]
- Polymers
- Metallurgy
- NIST Center for Neutron Research

Manufacturing Engineering Laboratory
- Precision Engineering
- Automated Production Technology
- Intelligent Systems
- Fabrication Technology
- Manufacturing Systems Integration

Building and Fire Research Laboratory
- Structures
- Building Materials
- Building Environment
- Fire Safety Engineering
- Fire Science

Information Technology Laboratory
- Mathematical and Computational Sciences[2]
- Advanced Network Technologies
- Computer Security
- Information Access and User Interfaces
- High Performance Systems and Services
- Distributed Computing and Information Services
- Software Diagnostics and Conformance Testing

[1] At Boulder, CO 80303.
[2] Some elements at Boulder, CO.

Semiconductor Measurement Technology:

Thin Film Reference Materials Development Final Report for CRADA CN-1364

Barbara J. Belzer, Keith Eberhardt,* Deane Chandler-Horowitz,
James R. Ehrstein, and Prabha Durgapal†

Semiconductor Electronics Division
Electronics and Electrical Engineering Laboratory

*Statistical Engineering Division
Information Technology Laboratory

National Institute of Standards and Technology
Gaithersburg, MD 20899-0001

†VLSI Standards, Inc.
San Jose, CAN 95134

April 1998

U.S. DEPARTMENT OF COMMERCE, William M. Daley, Secretary
TECHNOLOGY ADMINISTRATION, Gary Bachula, Acting Under Secretary for Technology
NATIONAL INSTITUTE OF STANDARDS AND TECHNOLOGY, Raymond G. Kammer, Director

National Institute of Standards and Technology Special Publication 400–100
Natl. Inst. Stand. Technol. Spec. Publ. 400–100, 42 pages (Apr. 1998)
CODEN: NSPUE2

U.S. GOVERNMENT PRINTING OFFICE
WASHINGTON: 1998

For sale by the Superintendent of Documents, U.S. Government Printing Office, Washington, DC 20402–9325

TABLE OF CONTENTS

LIST OF FIGURES

LIST OF FIGURES (Cont'd.) Page

LIST OF TABLES

Semiconductor Measurement Technology: Thin Film Reference Materials Development: Final Report for CRADA CN-1364

Barbara J. Belzer, Keith Eberhardt,[+] Deane Chandler-Horowitz, James R. Ehrstein,
Semiconductor Electronics Division
[+]Statistical Engineering Division
National Institute of Standards and Technology
Gaithersburg, MD 20899

Prabha Durgapal, VLSI Standards, Inc., San Jose, CA 95134

ABSTRACT

Independent single-wavelength ellipsometric measurements of thermally grown silicon dioxide thin films on silicon substrates and data analyses were compared between two laboratories (National Institute of Standards and Technology and VLSI Standards, Inc.) under a Cooperative Research and Development Agreement (CRADA). The primary intent, based on a sequence of sample exchanges, was to establish a measurement baseline enabling the demonstration of traceability to NIST for several silicon dioxide film thicknesses that are outside the range of Standard Reference Materials® (SRMs) available from NIST. Thin films less than 10 nm thickness were of particular interest. The results of the intercomparison show that there are small systematic differences in the values of the ellipsometric parameters Δ and ψ between the two laboratories along with occasional larger differences. Artificial differences in the calculated film thicknesses exist because of the use of different algorithms for computation. A single-layer model and a fixed value of the oxide index of refraction are assumed for the primary comparison in this collaboration; a two-layer model of the oxide/interface/substrate system is also presented.

Key words: calibration; ellipsometry; metrology; reference material; silicon dioxide; standards; thin films; traceability.

INTRODUCTION

The semiconductor industry makes much use of thin grown and deposited silicon dioxide films. There is a need for traceable film thickness artifact standards for the calibration of a wide range of optical instruments used for process development and monitoring of these films. In addition, there is a need to develop general, simple procedures to calibrate these instruments. Shrinking geometries and increasingly complex processes continue to place increasing demands on metrology equipment and associated standards.

The 1994 National Technology Roadmap for Semiconductors (NTRS), in place when this collaboration was initiated, envisioned the need for 4.5 nm gate oxides with a process tolerance of

±0.18 nm (3σ) at the 0.18 μm technology node (2001) [1]. The 1997 NTRS has moved this date up by several years. The microelectronics industry has requested that a standard with a nominal value of this order and an uncertainty lower than the process tolerance be developed to support the process equipment and instrumentation. In addition, current industry-wide adherence to the practices set forth in ISO 9000 and the certification of laboratories and processes under the auspices of those guidelines emphasize the need to have standards keep pace with the demands of the microelectronics industry.

While the relative process tolerances appear constant, changing manufacturing practices and methods continue to shrink the absolute value of the tolerances in the microelectronics industry at each technology node. The costs associated with the fabrication equipment and the metrology equipment which supports it are very high. It is an objective of NIST to provide standards and/or traceability at each of the processing nodes stated in the NTRS. The manner in which the NIST ellipsometrically characterized thin-film standards, Standard Reference Material (SRM®) Series 2530, have customarily been certified does not allow convenient recertification measurement on a single sample as is often required for ISO registration. The research and development for new standards is a time-consuming and costly process because it includes, aside from the metrology and data collection, characterization of the instrumentation used, collaboration with NIST statisticians for a complete analysis of errors and uncertainties, and a stringent peer review process. Therefore, the CRADA reported on here had a focus, as part of the collaboration, on the development of a more expedient approach to NIST traceable standards.

In 1988, after several years of research and development, NIST issued SRM® 2530-01 (50 nm), 2530-02 (100 nm), and 2530-03 (200 nm) which were measured using single wavelength ellipsometry. NIST has certified the ellipsometric parameters, values of the relative phase, Δ, and amplitude, ψ, the principal angle of incidence where $\Delta = 90°$, a derived film thickness based on a two-layer model of the dielectric film, and a calculated value for the refractive index of the silicon dioxide film [2]. The two-layer model includes a top layer of silicon dioxide and an interlayer, the composition and nature of which continues to be a research effort. The measurements were made using the ellipsometer specifically designed and built at NIST [3] with the intent to be able to obtain the most accurate ellipsometric parameters possible. A modeling method was developed concurrently to enable use of those data to determine the derived thickness and refractive index of the films thought to be most representative of the "true" values. The values presently certified by NIST obtained at the wavelength of 633 nm and the so-called principal angle of incidence, while believed to be very accurate, cannot presently be simply transferred or used to calibrate other instruments. These include spectroscopic and single-wavelength ellipsometers with the capability of either fixed or variable angle of incidence, reflectometers, and prism couplers.

Because ellipsometry does not directly measure a thickness, the problems associated with certification should not be underestimated. Depending on the method of ellipsometry used to determine the ellipsometric parameters, regardless of whether it is single-wavelength or spectroscopic, a variety of algorithms can be employed to calculate the thickness and refractive index of the material. The derived thicknesses and indices are highly dependent upon the layer structure assumptions and optical indices in the model applied and the algorithm used to adjust the model parameters to fit the data for the calculations [4,5].

Nominal thickness values for the current NIST certified standards include 10 nm, 14 nm, and 25 nm, in addition to the original 50 nm, 100 nm, and 200 nm SiO_2 films which were thermally grown on 76 mm diameter silicon substrates. The certified values and the method by which certification was achieved were developed at NIST [2]. Besides these certified values, supplemental, uncertified values of the derived film thickness based on a one-layer model are given. Also given are uncertified derived values of Δ and ψ for integer values of the angle of incidence, including 70°, based on the two-layer model and on the experimental Δ and ψ obtained at the principal angle. However, most instruments used to monitor industrial semiconductor thin-film processes cannot use the certified values directly. They rely on either the uncertified derived thickness based on the one-layer model or the uncertified values for Δ and ψ expected at integer values of the angle of incidence.

VLSI Standards, Inc. has been offering NIST-traceable film thickness standards (FTS) on a variety of substrate sizes for a number of years. They have also been providing a nontraceable reference material for 7.5 nm thick SiO_2 and plan to provide a traceable standard in that and thinner dielectric film regimes. Both NIST and VLSI Standards have recognized the need to provide state-of-the-art standards for the microelectronics industry in a timely manner. It was the intent of the collaboration in this Cooperative Research and Development Agreement (CRADA) between the Semiconductor Electronics Division at NIST and VLSI Standards, Inc. to develop and test artifacts with SiO_2 film thicknesses $\leq$10 nm and devise a method by which transferability and traceability could be more quickly and directly established and maintained for single wavelength ellipsometry measurements.

Overview of the CRADA Procedure

VLSI Standards manufactured and provided the artifacts used in this study, two each of nominally 4.5 nm, 7.5 nm, 10 nm, 50 nm, 100 nm, and 1000 nm thick oxides. Following the manufacture of the materials, VLSI Standards performed a number of measurements to ensure that the artifacts were of equal or better quality than their FTS series material. The artifacts were then sent to NIST for an initial round of measurements to gain familiarity with the artifacts, test and refine the NIST measurement protocol that would be required, and to establish a baseline for monitoring their stability. Upon completion of the initial round of NIST measurements and analysis, the staff from VLSI Standards and NIST met to discuss and agree upon the procedure for collecting the data and performing the analysis.

It was decided at that time (June 1996) to base the comparison on single-wavelength ellipsometry at 70° angle of incidence. The final report would include calculations based on a one-layer analysis of the dielectric layer using a refractive index of the SiO_2 layer of 1.460, the value used by VLSI Standards for their certification, and the silicon substrate optical constants, $n_{Si} = 3.875 - i0.0156$ [6]. The participants would perform data analysis using their own algorithm. Included in the analysis would be the film thicknesses of 7.5 nm, 10 nm, 50 nm, 100 nm, and 1000 nm. An analysis would also be made of the data obtained for the 4.5 nm oxide films and a determination made for the need to perform any additional data acquisition and analysis. Also, ancillary to this analysis, NIST would calculate thicknesses from the data obtained at each laboratory, utilizing common algorithms based on the described one-layer model and two-layer model using its software, MAIN1 [7]. A statistical analysis to evaluate the uncertainty of the observed differences between the two laboratories for the set of film thicknesses would be included in the report. The calculated thickness values from data

obtained by NIST at the individually determined principal angle of incidence, which is the protocol used in the certification of the NIST SRM 2530 series, were to be compared to the thicknesses calculated from the data obtained at the angle of incidence of 70°. It was also agreed that a mid-experiment statistical analysis would be performed to enable early detection of any problems with the measurement systems or artifact stability, or any needed revisions to the experiment design.

Experimental Design

Based on NIST's experience with interlaboratory studies [8], it was expected that an experimental design that incorporated several artifact exchanges, with relatively few measurements per exchange, would be appropriate for this study. The following sequence of measurements was agreed upon:

- The artifacts would be exchanged four to six times for measurements at each facility with no cleaning performed at either location other than using clean, dry, filtered nitrogen to remove dust particles.

- The artifacts would be measured at the center of the wafer over a 2- to 3-week period for each exchange, providing three to five independent measurements (e.g., all wafers would be independently mounted for each measurement) during that time.

- NIST would perform measurements at both the 70° angle of incidence, for use in direct comparison to the values obtained by VLSI Standards, and at the individually determined principal angle of incidence.

In fact, there were four exchanges of artifacts during the 6 months from June to December 1996, during which time five independent measurements were made on each sample during a 2- to 3-week time period.

The collaboration between NIST and VLSI Standards, by virtue of existing instrumentation at each laboratory, employed several ellipsometric methods: Conventional Null Ellipsometry (CNE) and Spectroscopic Ellipsometry (SE) were used at VLSI Standards, and Rotating Analyzer Ellipsometry (RAE) and Principal Angle-Rotating Analyzer Ellipsometry (PA-RAE) were used at NIST. The data were modeled to derive thicknesses and indices by several different methods as described above.

Materials Preparation

The silicon wafers that were used by VLSI Standards to manufacture the experimental artifacts met the SEMI Standard M1 Specifications for Polished Monocrystalline Silicon Wafers. The silicon material is 100 mm diameter, boron-doped, p-type <100> surface prime silicon. The resistivity range is 14 Ω•cm to 26 Ω•cm. The wafers were polished on one side only.

Two each of silicon dioxide films with the nominal thicknesses of 4.5 nm, 7.5 nm, 10 nm, 50 nm, 100 nm, and 1000 nm were manufactured. The silicon dioxide was grown at a temperature of 1000 °C in a purely dry 100% oxygen atmosphere. The time of growth was adjusted to yield different film thickness values. After oxidation, wafers with oxide thickness less than 10 nm were

annealed in nitrogen for 10 min and those with oxide thicknesses ≥10 nm were annealed for 20 min. Special care was taken to ensure consistent processing and film composition. The wafers carry an identification number and are not patterned in any way. These thicknesses were selected because the 10 nm, 50 nm, and 100 nm are all representative of existing NIST SRMs and very commonly used in the calibration of ellipsometers during installation and setup in a microelectronics fabrication or thin dielectric film research environment; the 7.5 nm value is currently offered by VLSI Standards as a non-traceable reference artifact and was the principal thickness of interest for the duration of this CRADA. The 4.5 nm thickness value was included as a research vehicle intended to begin evaluating the possibility of its certification and establishing its traceability to NIST in the very near future. The 1000 nm value was included to provide a measurement base for those film thicknesses beyond the first ellipsometric period (0 nm to ~290 nm). VLSI Standards also offers film thickness standards with nominal values of 285 nm, 400 nm, 675 nm, and 940 nm.

Sample Uniformity

Prior to using the samples for this CRADA, it was necessary to see if the oxide grown for different thickness values satisfied accepted typical industrial specifications. The samples selected were free of any contamination, microscopic defects, and cosmetic flaws. Following the visual inspection, the samples were inspected for flatness, uniformity, and manufacturing tolerances. In particular, the "uniformity" of the film thickness in the measurement region needed to satisfy the following criteria: oxide films with nominal thickness below 12 nm should vary by less than 0.2 nm, films with thickness 50 nm should vary by less than 0.6 nm, films with thickness of 1000 nm should vary by less than 2.0 nm over the measurement region, an area of 5 mm diameter in the wafer center.

Initial measurements were made at VLSI Standards to determine the uniformity for film thickness in the measurement area of the artifact. Uniformity was determined by both single wavelength ellipsometry utilizing the CNE method and SE.

Two sets of measurements were made on VLSI Standards' manual single-wavelength conventional-null ellipsometer (Rudolph Research Model 436 with a HeNe laser source)[1] immediately following oxidation, to ensure that the VLSI Standards uniformity criteria were satisfied. Two sets of measurements were also made on a commercial spectroscopic ellipsometer (SOPRA Model ES4G). Each set consisted of five measurement locations, one at the center and four at off-center points. The off-center points were located 2.5 mm from the center of the wafer. Table 1 shows measurement data together with the calculated values of thickness for the two measurement cycles made prior to the sample exchange. (The table in Appendix B lists the results of the spectroscopic measurements.) The measurement locations are given with the wafer flat at the bottom. Thickness values were calculated using a single-layer model. For the single-wavelength ellipsometer data analysis, the value of 1.460 was used for the refractive index of SiO_2 and the value of $3.875 - i0.0156$ was used for the complex refractive index of the silicon crystal substrate. The spectroscopic ellipsometer data analysis listed

[1]Certain commercial equipment, instruments, or materials are identified in this paper in order to adequately specify the experimental procedure. Such identification does not imply recommendation or endorsement by the National Institute of Standards and Technology, nor does it imply that the materials or equipment identified are necessarily the best available for the purpose.

in Appendix B uses the spectra of refractive indices for both SiO_2 and silicon crystal substrate from *The Handbook of Optical Constants of Solids*, E.D. Palik [9,10].

In Table 1, the parameter "nonuniformity" is defined as the difference between the maximum and minimum value of thickness calculated for a sample. The uniformity in the measurement region was determined to be in accordance with calibration requirements as employed by VLSI Standards, Inc.

Table 1: Single-Wavelength Uniformity Measurements Performed By VLSI Standards, Inc.

Run 1

	Thickness in Nanometers for Fixed Index of Refraction, n =1.460							
Wafer Serial Number	Center	Top	Bottom	Left	Right	Average	Non-uniformity	Standard Deviation
3723-001	4.89	4.90	4.89	4.89	4.92	4.90	0.03	0.01
3723-002	5.05	5.06	5.06	5.01	5.09	5.05	0.08	0.03
3722-001	7.55	7.54	7.55	7.56	7.53	7.55	0.03	0.01
3722-002	7.55	7.57	7.56	7.58	7.55	7.56	0.03	0.01
3721-001	10.47	10.47	10.48	10.47	10.53	10.48	0.06	0.03
3721-002	10.44	10.44	10.43	10.34	10.48	10.43	0.14	0.05
3365-003	49.67	49.66	49.7	49.7	49.68	49.68	0.04	0.02
3365-004	50.02	50.07	49.95	49.98	50.06	50.02	0.12	0.05
3718-001	99.09	98.99	99.2	98.95	99.24	99.09	0.29	0.13
3718-003	98.65	98.62	98.78	98.64	98.72	98.68	0.16	0.07
3562-005	1007.11	1006.62	1007.71	1007.41	1006.94	1007.16	1.09	0.42
3738-001	1034.43	1034.23	1034.61	1034.01	1034.8	1034.42	0.79	0.31

Run 2

	Thickness in Nanometers for Fixed Index of Refraction, n =1.460							
Wafer Serial Number	Center	Top	Bottom	Left	Right	Average	Non-uniformity	Standard Deviation
3723-001	5.06	5.07	5.05	5.04	5.08	5.06	0.04	0.02
3723-002	5.09	5.11	5.09	5.05	5.13	5.09	0.08	0.03
3722-001	7.60	7.60	7.59	7.62	7.59	7.60	0.03	0.01
3722-002	7.58	7.58	7.60	7.61	7.59	7.59	0.03	0.01
3721-001	10.51	10.51	10.51	10.48	10.55	10.51	0.07	0.02
3721-002	10.46	10.46	10.45	10.41	10.50	10.46	0.09	0.03
3365-003	49.73	49.72	49.77	49.77	49.71	49.74	0.06	0.03
3365-004	50.07	50.11	50.00	50.04	50.13	50.07	0.13	0.05
3718-001	98.96	98.96	98.99	98.94	99.15	99.00	0.21	0.09
3718-003	98.65	98.60	98.77	98.61	98.73	98.67	0.17	0.08
3562-005	1007.63	1007.09	1008.26	1007.80	1007.50	1007.66	1.17	0.43
3738-001	1034.62	1034.39	1034.93	1034.17	1034.94	1034.61	0.77	0.34

SAMPLE STABILITY BASELINE DETERMINATION

Upon receipt of the samples from VLSI Standards, NIST personnel began an extended series of

measurements using the NIST single-wavelength High-Accuracy Ellipsometer [3]. This instrument employs the photometric, rotating analyzer ellipsometric method in which the reflected beam goes through a rotating analyzer and the light intensity is measured by a silicon photodiode detector. The measurements were all made in the center of each wafer. Twenty-five Δ,ψ pairs at a NIST determined principal angle of incidence [11] and 16 Δ,ψ pairs at the industry-common angle of incidence of 70° were obtained on each sample between January 19, 1996 and February 28, 1996. This provided information for the baseline analysis of sample stability. Samples were sufficiently stable to proceed with the formal comparison.

Comparison of Ellipsometric Techniques (CNE, RAE, and PA-RAE)

Measurements in this study were made using both four-zone averaged CNE at VLSI Standards Inc. and RAE at NIST. NIST also made use of Principal Angle-Rotating Analyzer Ellipsometry (PA-RAE) in which the principal angle of incidence for each sample is determined experimentally and is defined as that angle where the ellipsometric parameter $\Delta = 90°$. For this condition, the ellipsometric parameter ψ equals the polarizer azimuth angle. At these conditions, the reflected light is circularly polarized, there is greater sensitivity to very small changes in the subject sample, and optimally accurate data can be obtained for analysis.

CNE always uses a compensator, or quarter-wave plate (QWP), thus limiting its use to a single wavelength. Manual null ellipsometry is time-consuming but can greatly reduce systematic errors due to aberrations in the optical elements with appropriate zone averaging [12]. In general, though, the RAE with one polarizer and analyzer has fewer optical aberrations than the CNE with its additional QWP. Both RAE and CNE have regions of high measurement uncertainty in Δ. In the RAE, measurement ambiguities occur when $\Delta = 0°$ or 180°. The linearity of the detector in the RAE is important especially for fully modulated signals. With the CNE, there are measurement ambiguities when $\psi = 0°$ or 90°. These problems are further illustrated and discussed below.

Ellipsometry is based on the analysis of the relative change in polarization of light, polarized parallel, *p*, and perpendicular, *s*, to the plane of incidence upon reflection from a surface. The Fresnel reflection coefficients, i.e., the ratio of the reflected electric field vector to the incident electric field vector, is R_p for the parallel polarization and R_s for the perpendicular polarization. The complex ratio of total reflection, ρ, which relates the measured ellipsometric parameters Δ and ψ to the material parameters contained in R_p and R_s, can be written as

$$\rho = \frac{R_p}{R_s} = \tan\psi e^{i\Delta} \qquad (1)$$

A subsequent series of calculations ultimately results in the determination of thickness and refractive index values for the film.

CNE (Conventional Null Ellipsometry)

For CNE, the following equation governs the light intensity and is used to determine Δ and ψ:

$$I_{CNE}=\frac{I_0(|R_p|^2+|R_s|^2)[1-\cos 2\psi\cos 2A+\sin 2\psi\sin(\Delta-2P)\sin 2A]}{4}, \quad (2)$$

where P and A are the Polarizer and Analyzer azimuth angles and I_0 is the light intensity through the polarizer with the compensator or quarter wave plate fixed at ±45° prior to the reflection of light from the sample surface.

The intensity has a minimum which can be approached by independently rotating both the polarizer and the analyzer to get the null conditions

$$P_{null}=\frac{\Delta}{2}\pm\frac{\pi}{4}, \quad (3)$$

$$A_{null}=\psi. \quad (4)$$

Near null, $P = P_{null} + \delta P$, $A = A_{null} + \delta A$ and $|\delta P|$, $|\delta A|$ are $<<1$; then the intensity near null for the CNE can be expressed as

$$I_{CNE}=\frac{I_0(|R_s|^2+|R_p|^2)[(\delta A)^2+(\delta P)^2\sin^2 2\psi]}{2}. \quad (5)$$

Thus, the intensity has a parabolic variation in δP and δA. These variations are independent of each other. Equation (5) shows that I_{CNE} is insensitive to δP and therefore Δ when $\psi = 0°$ or $90°$ ($\sin^2 2\psi = 0$).

RAE (ROTATING ANALYZER ELLIPSOMETRY)

The photometric method does not require a null measurement. The intensity varies with the analyzer's azimuth, A:

$$I_{RAE}=\frac{I_0(|R_s|^2\sin^2 P+|R_p|^2\cos^2 P)(1+\alpha\cos 2A+\beta\sin 2A)}{2}, \quad (6)$$

where

$$\alpha = \frac{\tan^2\psi - \tan^2 P}{\tan^2\psi + \tan^2 P}, \tag{7}$$

$$\beta = \frac{2\tan\psi\tan P\cos\Delta}{\tan^2\psi + \tan^2 P}. \tag{8}$$

The parameters α and β can be determined from a Fourier analysis of the modulating intensity of the rotating analyzer signal. In the case of the NIST ellipsometer, the rotating analyzer is housed in an optical encoder which provides the computer with an accurate read-out of its position for use in the processing of the intensity signal.

Because most commercially available single-wavelength systems are utilized at the fixed angle of incidence of 70°, NIST RAE measurements were made at this angle for a more direct comparison between the two laboratories in this study. Unfortunately, for the samples with film thicknesses of <10 nm, this results in a Δ value close enough to 180° where the reflected light is more linearly polarized than is desirable for RAE analysis because of errors associated with detector nonlinearity.

PA-RAE (PRINCIPAL ANGLE ROTATING ANALYZER ELLIPSOMETRY)

In this adaptation of the RAE method, the angle of incidence is set close to the *principal angle*, which changes as a function of oxide thickness. The NIST Rotating Analyzer Ellipsometer has a nearly continuous (±0.001°) step size for the angle of incidence. Utilizing this ac null method results in nearly circularly polarized light, which gives optimum measurement conditions [13].

In PA-RAE ellipsometry, P, which is the polarizer azimuth with respect to the plane of incidence, is set to ψ, while Δ is set to 90° by varying the angle of incidence to be close to the principal angle. As seen in eqs (7) and (8), the ac null signal obtained in this method occurs when both α and $\beta = 0$. The advantage gained in utilizing the PA-RAE is that systematic errors related to photometry are eliminated. The greatest disadvantage is that it is difficult and time-consuming to ensure accurate setting of the angle of incidence. The NIST system was designed to minimize the former disadvantage by the use of calibrated rotation stages [14].

The value of ψ at the principal angle of incidence for SiO_2 under 10 nm in thickness becomes close enough to zero that there is an attenuation of the signal to the point where the amplifier gain sensitivity must be increased, thus decreasing the signal-to-noise ratio. At 70° angle of incidence, subsequent ψ values are larger, allowing for greater intensity at the detector and a better signal-to-noise ratio than for PA-RAE at these thicknesses. The tradeoff is then that at 70° angle of incidence, the value for Δ is close to 180° which indicates that, rather than circularly polarized light, it is nearly linearly polarized, and far from optimum [13]. Again, when eqs (6), (7), and (8) are examined, the optimum measurement conditions for photometric ellipsometry occur when $\alpha = \beta = 0$ which represents circularly polarized light.

Principal angle measurements were included in the experiment to provide what is believed to be the most accurate data possible for analysis. These measurements also provided experimental information for a comparison of the results of data obtained at the Principal Angle measurement angle traditionally used by NIST in certifying the SRM 2530 series and the 70° angle readily accessible in the commercial setting.

Regardless of the method or the modeling algorithm used, it is of primary importance to remember that any measurement uncertainties, both systematic and random, will propagate through the calculations to the final result. This means that the total uncertainties associated with a derived thickness and refractive index represent the accumulation of uncertainties present at each intermediary step, thus compounding those inherent in the mathematical code and in the measurement system itself.

RESULTS AND DISCUSSION

While there was some indication of sample thickness change during the 6 months of the formal test, this observation was not found to be supported by most of the data acquired, and it must be concluded that there was no sample drift within the level of reproducibility of the data accumulated.

During the four exchanges of the samples between the laboratories for the formal measurements, there were instances indicating possible loss of statistical control. However, because there were only four exchanges, there were insufficient total data to make sound statistical inference regarding individual measurement sets. It was decided to include all data in the final analysis rather than reduce the number of degrees of freedom through data elimination.

COMPARISON OF Δ AND ψ

The grand average values of Δ and ψ experimentally obtained at an angle of incidence of 70° were compared for the four sample exchanges. Detailed tables of all individual measurements are given in Appendix 3. It should be noted that Δ and ψ are nonlinear functions of sample thickness, wavelength, angle of incidence, polarizer azimuth, the properties of the optical elements in the ellipsometer, and the sample alignment which can in turn cause errors in the angle of incidence. In particular, sample alignment errors can be random or systematic and may account for some of the differences observed between the laboratories for Δ and ψ.

The general results for the calculated differences in Δ and ψ in Tables 2 and 3 show differences in Δ approaching 0.3°, with the largest differences occurring for the thinnest oxides, while the differences for ψ are on the order of 0.1°. Several modeling calculations were made to see whether differences of these magnitudes could be explained by simple assumptions without going into detailed considerations about aberrations in the optical components of the instruments, which is beyond the intended scope of this comparison study.

Table 2: Measured values of Δ at AI = 70°

Δ in Degrees						
Sample I.D.	Nominal Thickness (nm)	Mean Values		Difference VLSI-NIST		Expanded Unc. of Difference
		VLSI	NIST			
3723-001	4.5	164.58	164.86	-0.28		0.35
3723-002	4.5	164.46	164.70	-0.23		0.36
3722-001	7.5	157.74	157.88	-0.14		0.23
3722-002	7.5	157.71	157.86	-0.15		0.21
3721-001	10	150.31	150.54	-0.23	*	0.14
3721-002	10	150.54	150.68	-0.14		0.15
3365-003	50	95.51	95.55	-0.04		0.05
3365-004	50	95.35	95.39	-0.04		0.09
3718-001	100	78.93	78.90	0.02		0.05
3718-003	100	78.90	78.85	0.05		0.07
3562-005	1000	-86.16	-86.19	0.04		0.16
3738-001	1000	-79.97	-80.07	0.10	*	0.04

* Denotes differences that are larger, in absolute value, than their expanded uncertainties

[Due to numerical roundoff, listed differences may differ in the last digit from what would be obtained by subtracting the listed mean values.]

Table 3: Measured Values of ψ at AI = 70°

ψ in Degrees						
Sample I.D.	Nominal Thickness (nm)	Mean Values		Difference VLSI-NIST		Expanded Unc. of Difference
		VLSI	NIST			
3723-001	4.5	10.71	10.79	-0.08	*	0.05
3723-002	4.5	10.72	10.80	-0.08	*	0.04
3722-001	7.5	11.01	11.09	-0.08	*	0.04
3722-002	7.5	11.02	11.09	-0.08	*	0.04
3721-001	10	11.47	11.55	-0.07	*	0.04
3721-002	10	11.45	11.54	-0.09	*	0.05
3365-003	50	22.74	22.86	-0.12	*	0.09
3365-004	50	22.82	22.93	-0.11	*	0.08
3718-001	100	40.77	40.82	-0.06		0.10
3718-003	100	40.58	40.66	-0.08		0.11
3562-005	1000	62.34	61.99	0.34	*	0.14
3738-001	1000	39.87	39.94	-0.07		0.13

* Denotes differences that are larger, in absolute value, than their expanded uncertainties

[Due to numerical roundoff, listed differences may differ in the last digit from what would be obtained by subtracting the listed mean values.]

Figures 1 and 2 result from simple model calculations and indicate how much Δ and ψ might change, or be in error, as a function of oxide layer thickness, resulting from either of two simple sources of variation that might have been encountered in this measurement sequence. Figure 1 shows how an error of just 0.05° in the angle of incidence at a nominal angle setting of 70° would affect Δ and ψ as a function of thickness. Figure 2 shows the changes in Δ and ψ that would occur as a function of thickness resulting from just a 0.1 nm increase in film thickness; this could result from any surface contamination layer with an index of refraction similar to that of the SiO_2, e.g., n = 1.3 to 1.6, and could include less than a monolayer of moisture or organic contamination. Both examples show that it is possible to incur offsets of about the magnitude seen in Tables 2 and 3 through some very simple mechanisms.

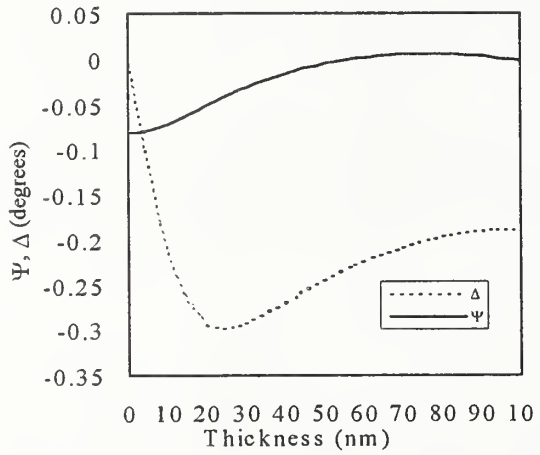

Figure 1. Change in Δ and ψ with a 0.05° change from 70° in the angle of incidence for different SiO_2 film thicknesses.

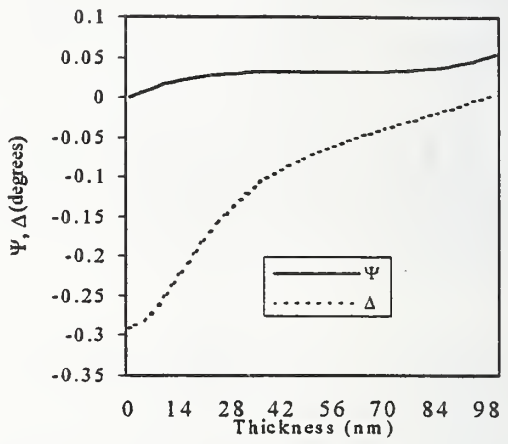

Figure 2. Change in Δ and ψ with a 0.1 nm change in the thickness of oxide film at 70° angle of incidence for different film thicknesses.

Δ Values Measured By NIST and VLSI Standards at 70° Angle of Incidence

The measured values of Δ obtained by the two labs are compared in Table 2. In this table, the grand mean values of Δ are shown for each of the 12 artifacts. For each artifact, the difference between VLSI Standards and NIST is shown in the fifth column, along with the calculated expanded uncertainty of the difference in the sixth column. The method of calculating the expanded uncertainties for Tables 2 to 6 is described in Appendix A.

For films below about 50 nm in thickness, the VLSI Standards measured values of Δ tend to be lower than the corresponding values for NIST. For the 100 nm and 1000 nm thicknesses, VLSI Standards' measured Δs were higher than NIST's. In two cases, samples 3721-001 and 3738-001, the differences were "statistically significant" in that the differences of the mean values were larger, in absolute value, than the expanded uncertainty values (95% statistical confidence limits). The offsets noted in this table are consistent with errors or offsets in the angle of incidence as illustrated in Figures 1 and 2 and described above. The experimental offsets in Δ have values that depend on thickness in a manner very similar to that shown in Figure 2 due to a 0.1 nm increase in film thickness. While experimental results do not support evidence of an accumulation of organic contamination, there is a possibility that variations in the atmospheric conditions (e.g., relative humidity) may cause a small fluctuation in thickness.

Ψ Values Measured By NIST and VLSI Standards at 70° Angle of Incidence

The measured values of ψ obtained by the two labs are compared in Table 3. The table shows the grand mean values of ψ for each of the 12 artifacts, and for each artifact, the difference between VLSI Standards and NIST is shown, along with the calculated expanded uncertainty of the difference.

Except for artifact 3562-005, the values of ψ obtained by VLSI Standards tend to be about 0.1° lower than those obtained by NIST. These results are not simply explained by an assumption of a small difference in angle of incidence as shown in Figure 1. For thicknesses of 50 nm or less, the differences are statistically significant in that the observed differences are larger, in absolute value, than the corresponding expanded uncertainties (95% statistical confidence limits). However, for the three thinnest film categories, $\leq$10 nm, there is very little sensitivity of the calculated film thickness to the value for ψ. In the exceptional case of the 1000 nm artifact 3562-005, the VLSI Standards mean value is larger than the NIST mean by +0.34°. This reflects a distinctive physical property of this artifact in that its nominal, calculated thickness of 1008 nm, a fourth cycle thickness, corresponds to a first cycle thickness of ~158 nm. This thickness has the distinction of falling on a part of the curve as depicted in Figure 3, where the slope of the polarizer azimuth angle versus thickness and, hence, corresponding ψ value is extremely steep, causing a marked sensitivity to variations in the measurements. It is in this area where any variation in instrumentation, optical components and their housings, as well as variation in the actual measurements caused by individual alignment of the sample on the system would logically appear as a significant difference in the measured values reported by the individual laboratories.

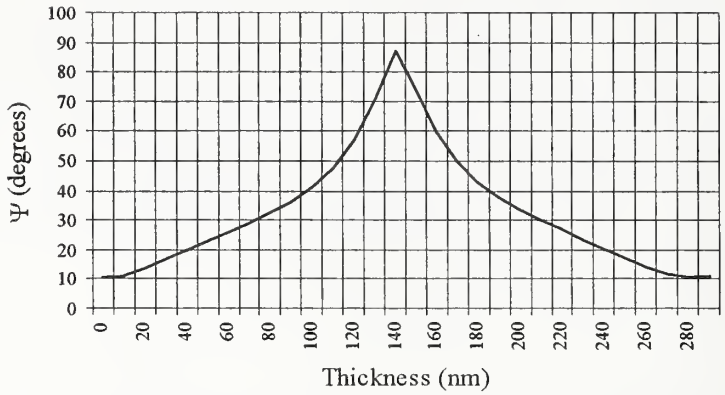

Figure 3: ψ Values at 70° Angle of Incidence
First Thickness Cycle
$\lambda = 632.8$, $n_f = 1.460$

FILM THICKNESS AND MODELING

The model and analysis used in the calculation of thickness and refractive index is as equally important as the accuracy of the measurements themselves. The resultant data presented in the preceding sections were examined in several different ways described below.

ONE-LAYER MODEL, 70° ANGLE OF INCIDENCE AND PRINCIPAL ANGLE OF INCIDENCE

The one-layer, fixed refractive index model calculated using the individual algorithms employed by VLSI Standards and by NIST was examined. This constitutes the most direct comparison between the derived thickness values that would be produced by each lab, in isolation, for these artifacts. A second comparison considers the results after recalculating the data acquired by VLSI Standards using the NIST analysis program, MAIN1. This was done specifically to begin to understand any observed differences in calculated thickness due to the algorithm as opposed to instrument and/or technique (CNE vs. RAE).

Table 4 shows a comparison of the calculated thickness values obtained by VLSI Standards and NIST, using their own standard algorithm for the calculation. These values are graphically depicted in Figure 4. In each case, the same set of fixed parameters was used for the calculation (refractive indices of air, SiO_2, and Si), together with the individual laboratory's measured values of Δ and ψ.

Table 4: Calculated Thickness (one-layer model, using own algorithms)

Thickness (nm)						
Sample I.D.	Nominal Thickness (nm)	Mean Values		Difference VLSI-NIST		Expanded Unc. of Difference
		VLSI	NIST			
3723-001	4.5	5.18	5.10	0.08		0.12
3723-002	4.5	5.23	5.16	0.07		0.13
3722-001	7.5	7.71	7.69	0.02		0.09
3722-002	7.5	7.73	7.70	0.03		0.08
3721-001	10	10.63	10.58	0.05		0.06
3721-002	10	10.53	10.52	0.01		0.08
3365-003	50	49.86	50.11	-0.26	*	0.11
3365-004	50	50.10	50.33	-0.23	*	0.12
3718-001	100	99.19	99.25	-0.06		0.18
3718-003	100	98.85	98.95	-0.11		0.19
3562-005	1000	1007.89	1008.09	-0.20	*	0.11
3738-001	1000	1034.83	1034.67	0.16		0.27
* Denotes differences that are larger, in absolute value, than their expanded uncertainties						

[Due to numerical roundoff, listed differences may differ in the last digit from what would be obtained by subtracting the listed mean values.]

From this comparison, the mean thickness values for the artifacts ≤10 nm, as well as the 100 nm film artifacts, differ by an average of <0.1 nm. For the artifacts ≤10 nm, the VLSI Standards measurements and calculations result in slightly larger thickness values than obtained by NIST, while for 50 nm and 100 nm films, the situation is reversed with VLSI Standards calculations, resulting in lower thickness values than NIST. For the 50 nm artifacts, the VLSI Standards method results in thickness values that are lower than NIST's by about 0.25 nm, and the differences are statistically significant in that they exceed the corresponding expanded uncertainties. The same applies to the 1000 nm artifact 3562-005, where the VLSI Standards' thickness is lower than NIST's by 0.2 nm. Again, the difference is statistically significant, implying that it cannot plausibly be explained as a result of random measurement error. However, it should be noted that the functional agreement ≤0.2 nm for the 1000 nm samples in this study regardless of the algorithm used represents an agreement within such a small percentage (0.02%) of the total thickness, that it is adequate for this thickness regime and the purposes of this study. No further calculations were done on the 1000 nm films.

In interpreting determinations of "statistical significance," it is important to keep in mind that statistical significance is not related to the practical importance of a quantity. The statistical significance of an observed difference only addresses the question of whether the observed value differs from zero by more than its uncertainty. In informal terms, it addresses the question of whether the uncertainty in a given experimental result is small enough to "prove" (at the 95% level of confidence) that the long term systematic offset of the two measurement systems is something other than exactly zero. Metrology experience indicates that, given enough experimentation, any two measurement systems can be shown to have some nonzero amount of systematic offset. On the other hand, a small number of experimental measurements, with large uncertainties, might fail to show statistical significance for a difference that could be quite large. Thus, it is more meaningful to

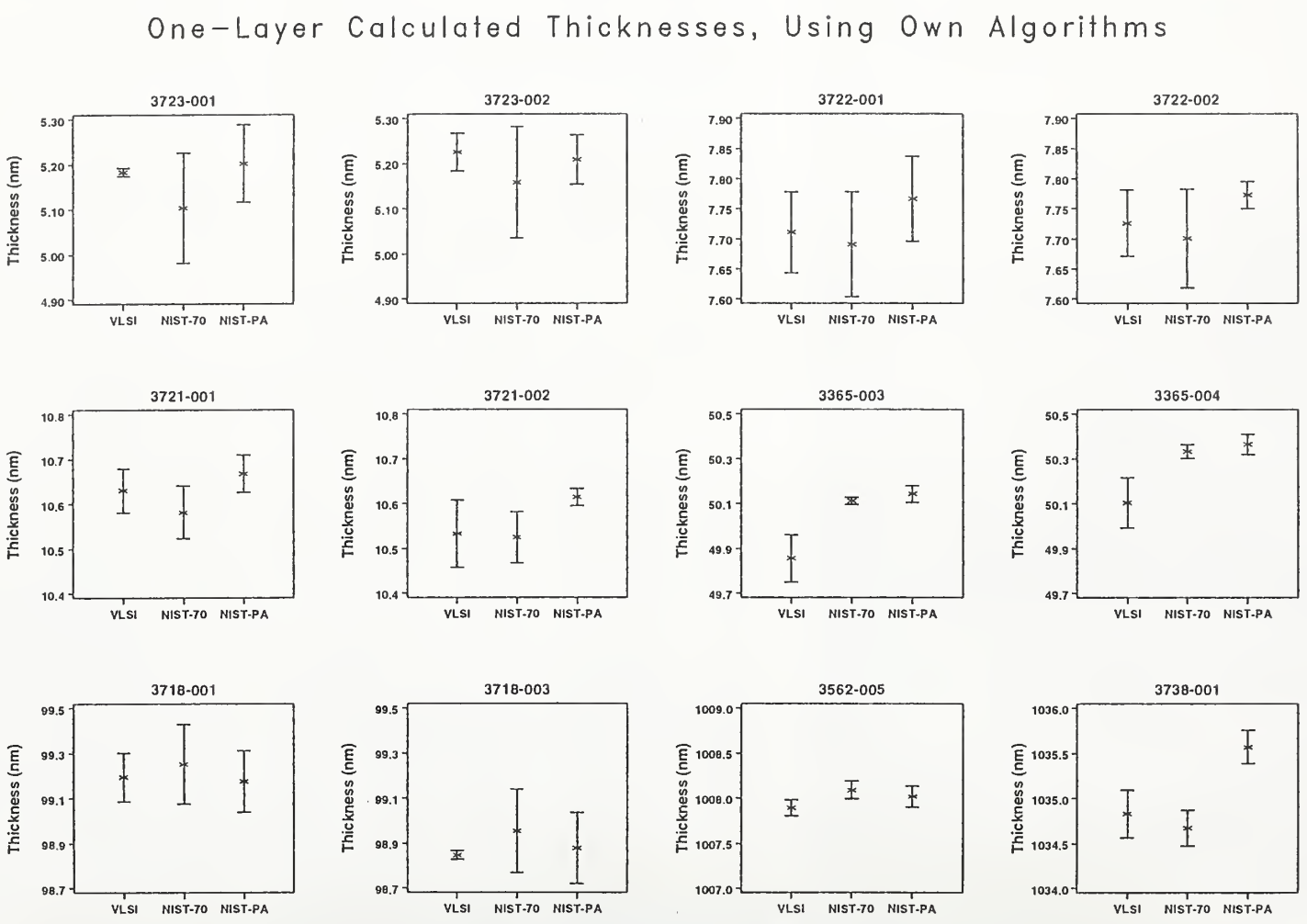

Figure 4. Comparison of calculated one-layer thickness values for three measurement methods: VLSI Standards at 70° angle of incidence, NIST at 70° angle of incidence, and NIST at the principal angle.

consider what can be said, on the basis of the present comparison, about the maximum possible size of the (presumed non-zero) systematic offset between the two measurement systems studied.

In particular, it is of interest to consider what can be said, on the basis of Table 4, about the possible size of the overall systematic offset between the VLSI Standards and NIST measurement systems. Since the thicknesses in Table 4 were calculated by the algorithm that is routinely used in each laboratory, the differences shown there reflect a realistic comparison of the calculated thicknesses that would result from routine application of the current measurement systems, including data reduction methods.

At the 95% confidence level, an upper limit to the long-term average difference, or systematic offset, between the two measurement systems is given by the sum of the observed mean difference (in absolute value), plus the expanded uncertainty in Table 4. This sum is 0.2 nm or less for all artifacts having nominal film thicknesses of 10 nm or less. That is, the results shown in Table 4 show that the systematic offset between the two measurement systems (including thickness calculation algorithms) is less than or equal to 0.2 nm for film thicknesses of 10 nm or less. As a whole, one can say, at the 95% level of confidence, that the (absolute value of the) systematic offset is no greater than 0.37 nm for artifacts with film thicknesses of 100 nm or less, and no greater than 0.43 nm for all artifacts studied.

Principal Angle Measurements

The comparison of calculated thicknesses can be extended by incorporating the thickness values obtained from the NIST principal angle measurements with the calculated thicknesses obtained from the VLSI Standards and NIST 70° angle of incidence measurements. NIST has based the certified values of the existing series of SRMs® on the measurements made at the Principal Angle of Incidence based on work showing them to be the most accurate. Figure 4 shows the graphical comparison. The error bars in the plot represent 95% statistical confidence limits, calculated from the reduced data set consisting of four values of the mean thickness per exchange for each artifact and measurement method. In the figure, artifacts for which the error bars for VLSI Standards and NIST 70° do not overlap correspond to cases in Table 4 where the difference between the VLSI Standards and NIST 70° mean values show a statistically significant difference.

The differences in Table 4 reflect the combined effect of differences between the two laboratories' measurement systems and also between two separate calculation algorithms. In order to focus on just the differences due to the measurement systems, the film thickness values were recalculated, from VLSI Standards' raw Δ and ψ data, using NIST's standard algorithm as embodied in the MAIN1 program. Because the MAIN1 algorithm is not written to converge on data taken on thicknesses outside the first ellipsometric cycle (0 nm to 290 nm), this comparison was only carried out for the 100 nm and thinner films. The results of this comparison are summarized below in Table 5.

Table 5: Calculated Thickness (one-layer model, both using MAIN1)

Thickness (nm)						
Sample I.D.	Nominal Thickness (nm)	Mean Values		Difference VLSI-NIST		Expanded Unc. of Difference
		VLSI	NIST			
3723-001	4.5	5.20	5.10	0.10		0.13
3723-002	4.5	5.24	5.16	0.08		0.13
3722-001	7.5	7.74	7.69	0.05		0.09
3722-002	7.5	7.76	7.70	0.06		0.08
3721-001	10	10.67	10.58	0.09	*	0.06
3721-002	10	10.58	10.52	0.06		0.06
3365-003	50	50.09	50.11	-0.02		0.08
3365-004	50	50.32	50.33	-0.01		0.12
3718-001	100	99.15	99.25	-0.10		0.17
3718-003	100	98.81	98.95	-0.14		0.19
* Denotes differences that are larger, in absolute value, than their expanded uncertainties						

The comparison in Table 5 shows that the mean thickness values differ by 0.1 nm or less for all artifacts with film thickness less than or equal to 50 nm. In fact, a major difference between Tables 4 and 5 is that the 50 nm films showed the largest differences in Table 4 (where separate calculation algorithms were used) and the smallest differences in Table 5 (where the same algorithm is used for both measurement methods). In Table 5, the VLSI Standards measurement data produce higher thickness values for the artifacts with the three thinnest films (less than or equal to 10 nm) and lower thickness values for the thicker films (50 nm and 100 nm). The only statistically significant difference in mean thickness values occurs for artifact 3721-001, with a 10 nm film, which was also the only artifact to show statistically significant differences in both Δ and ψ in Tables 2 and 3, respectively.

For this comparison, differences attributable to the algorithm employed in calculating the thickness are not found to be a significant contributor to measurement differences except for the 50 nm samples. The differences arise because the measured Δ and ψ values do not fit the film substrate model exactly, experimental errors exist, and the programs are calculating a "best fit" value for the thickness based on their own algorithms. The algorithms used by VLSI Standards and NIST differ in the functions used in minimization. The algorithm employed by NIST uses the sum of the squares of the differences between the measured and modeled values of Δ and ψ. Constraints on the minimization function include the fixed index of refraction of the SiO_2 layer. The results in Table 5 can be used to derive an upper bound for the systematic offset between the two measurement systems, assuming that both were using the MAIN1 algorithm for one-layer thickness calculations. At the 95% confidence level, an upper bound for the systematic offset is obtained by adding the (absolute) differences to their corresponding expanded uncertainties. This yields the statement that the systematic offset is no larger (in absolute value) than 0.23 nm for nominal film thicknesses of 50 nm or less, and no larger than 0.31 nm for thicknesses of 100 nm or less. The results shown in Table 5 for a common data reduction algorithm are depicted graphically in Figure 5, together with the corresponding PA measurements (as in Fig. 4).

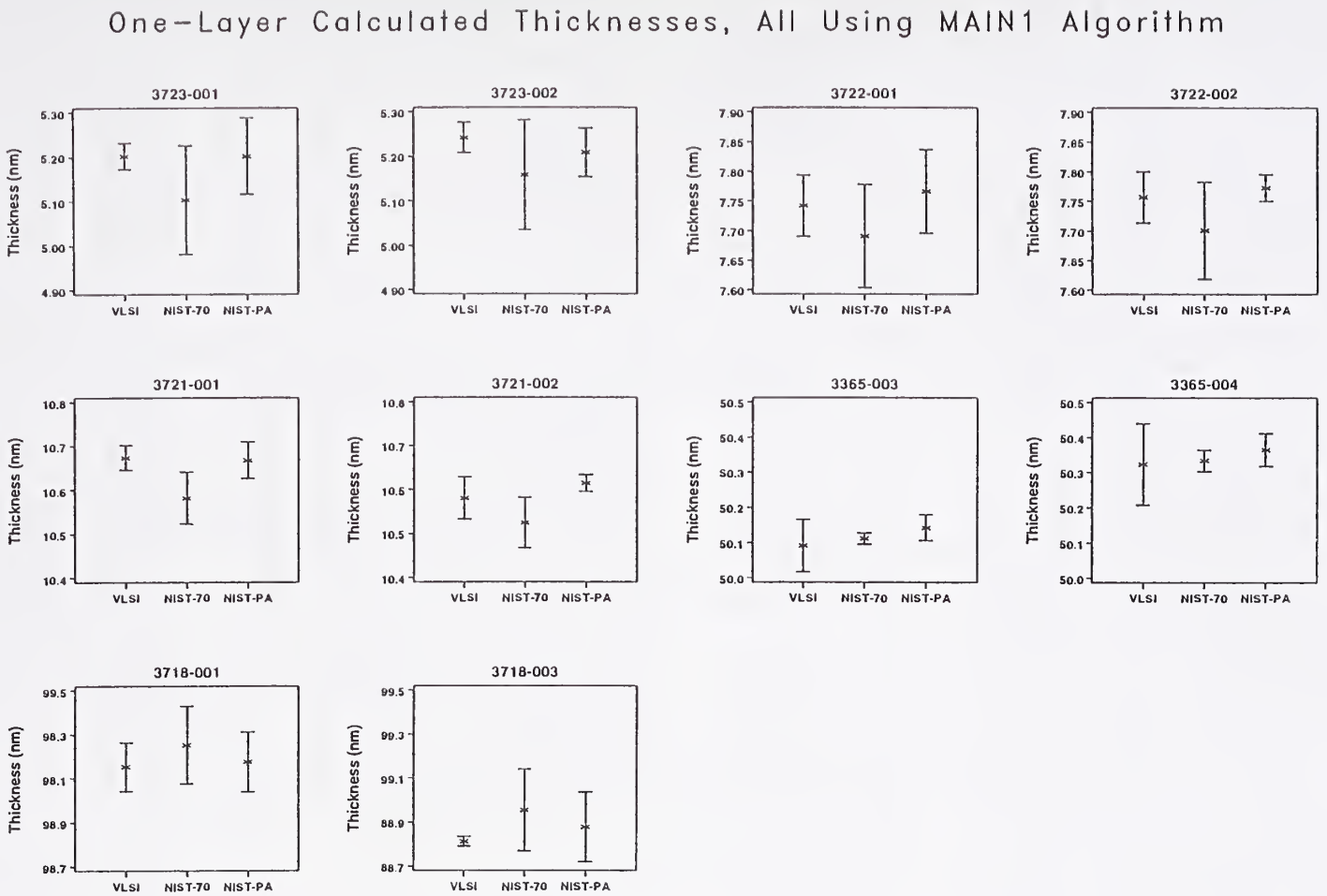

Figure 5. Comparison of calculated one-layer thickness values, all calculated using the MAIN1 algorithm. The Δ and ψ values were obtained by three measurement methods: VLSI Standards at 70° angle of incidence, NIST at 70° angle of incidence, and NIST at the principal angle.

COMPARISON OF CNE, RAE, AND PA-RAE ONE-LAYER CALCULATED THICKNESS

A direct comparison of the two thickness calculation algorithms can be made by comparing, for each measured (Δ,ψ) pair, the calculated thickness obtained from the VLSI Standards algorithm and that obtained from MAIN1. For each artifact, there are 20 measurements available for this comparison. Figure 6 shows the 20 differences, obtained by subtracting the MAIN1-calculated thickness from the corresponding VLSI Standards-calculated thicknesses, for ten artifacts with film thicknesses up to 100 nm. The plot shows that the VLSI Standards algorithm gives thickness values that are uniformly slightly lower than those obtained from MAIN1 for the artifacts with nominal thicknesses of 4.5 nm, 7.5 nm, and 10 nm. For the 50 nm artifacts, the difference between the two algorithms is greater, with VLSI Standards producing results that average a little more than 0.25 nm below the MAIN1 values. The variability of the differences is also larger for 50 nm thicknesses than for the others. The sign of the differences reverses for the 100 nm films, with the VLSI Standards algorithm producing slightly higher results than MAIN1 in that case.

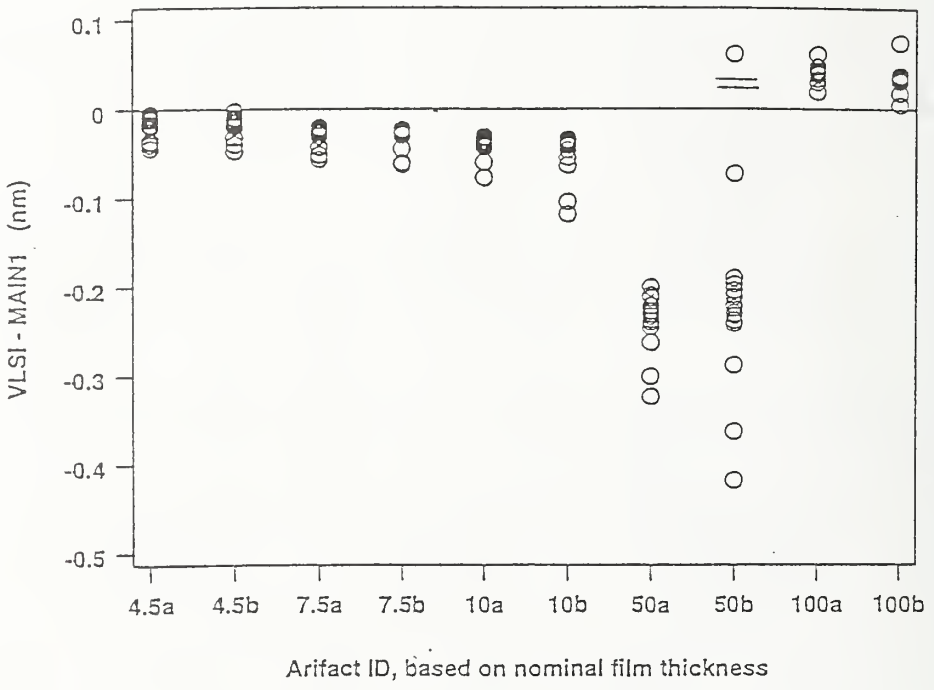

Figure 6. Comparison of two algorithms for calculating thicknesses, using the VLSI Standards (Δ,ψ) data. For each (Δ,ψ) pair, both VLSI Standards' algorithm and NIST's MAIN1 algorithm were used to calculate one-layer thickness values. The plot shows the differences, VLSI−MAIN1, between the resulting calculated values for the 20 measurements of each artifact. The artifacts are labeled by their nominal thicknesses in the order shown in Table 4; for example, artifact 3723-001 is designated 4.5a, and 3723-002 is 4.5b, etc.

TWO-LAYER MODEL, 70° ANGLE OF INCIDENCE AND PRINCIPAL ANGLE OF INCIDENCE

This comparison uses the data acquired and models a thickness and refractive index of the film based on a two-layer model. The two-layer model calculations were implemented using NIST's MAIN1 computer program. This program generates values of film thickness, t_f, and interlayer thickness, t_i, along with derived values of the refractive indexes for the film and the interlayer by doing a batch analysis of all thicknesses. A two-layer model has been found to give a fit simultaneously to all samples that is much better than the one-layer model [2]. The one-layer model, when varying both n and t, tends to give an index value that varies with film thickness. Table 6 gives a numerical comparison of the two-layer thickness values obtained from the VLSI Standards and NIST 70° Δ and ψ data. In this table, two-layer thickness is defined as the sum of the film thickness and the interlayer thickness obtained from the two-layer calculation: $thickness = (t_f + t_i)$. The grand average refractive index of the SiO_2 ,n_f, for the collective NIST batches was calculated to be 1.464 with grand average interlayer thickness, t_i, of 0.91 nm with an interlayer refractive index, $n_i = 2.8$. The corresponding values for the collective VLSI Standards batches were calculated to be 1.464 and 0.95 nm, respectively, and the interlayer refractive index, n_i, of 2.8. By analyzing measurements made at the principal angle of incidence along with the calculated thicknesses and comparing the results with those obtained at the 70° angle of incidence from both laboratories, a perspective can be gained for the degree of difference that the method and modeling can have on the final outcome as shown in Figure 7. The grand averages for the refractive index for the SiO_2 film, n_f, the interlayer thickness, t_i, and an interlayer refractive index, n_i, calculated from the batches of principal angle data from NIST are 1.464, 0.73 nm, and 2.8, respectively.

Table 6: Calculated Thickness (two-layer model)

Thickness (nm)						
Sample I.D.	Nominal Thickness (nm)	Mean Values		Difference VLSI-NIST		Expanded Unc. of Difference
		VLSI	NIST			
3723-001	4.5	5.28	5.15	0.13		0.17
3723-002	4.5	5.32	5.21	0.11		0.17
3722-001	7.5	7.80	7.72	0.08		0.12
3722-002	7.5	7.82	7.73	0.09		0.13
3721-001	10	10.72	10.59	0.13	*	0.11
3721-002	10	10.62	10.53	0.09		0.10
3365-003	50	49.78	49.73	0.05		0.11
3365-004	50	50.01	49.95	0.06		0.11
3718-001	100	99.22	99.15	0.07		0.55
3718-003	100	98.87	98.84	0.03		0.54
* Denotes differences that are larger, in absolute value, than their expanded uncertainties						

In this comparison, almost all the artifacts have mean differences of 0.1 nm or less. Interestingly, the thickness values obtained from the VLSI Standards data are all larger than the corresponding NIST values. As was true in Table 5, the only artifact showing a statistically significant difference is 3721-001, with a 10 nm film, and for which the mean values for both Δ and ψ showed statistically significant differences in Tables 2 and 3. It is not within the scope of this report to examine the details of the two-layer model analysis, but the results are included for an illustration of the

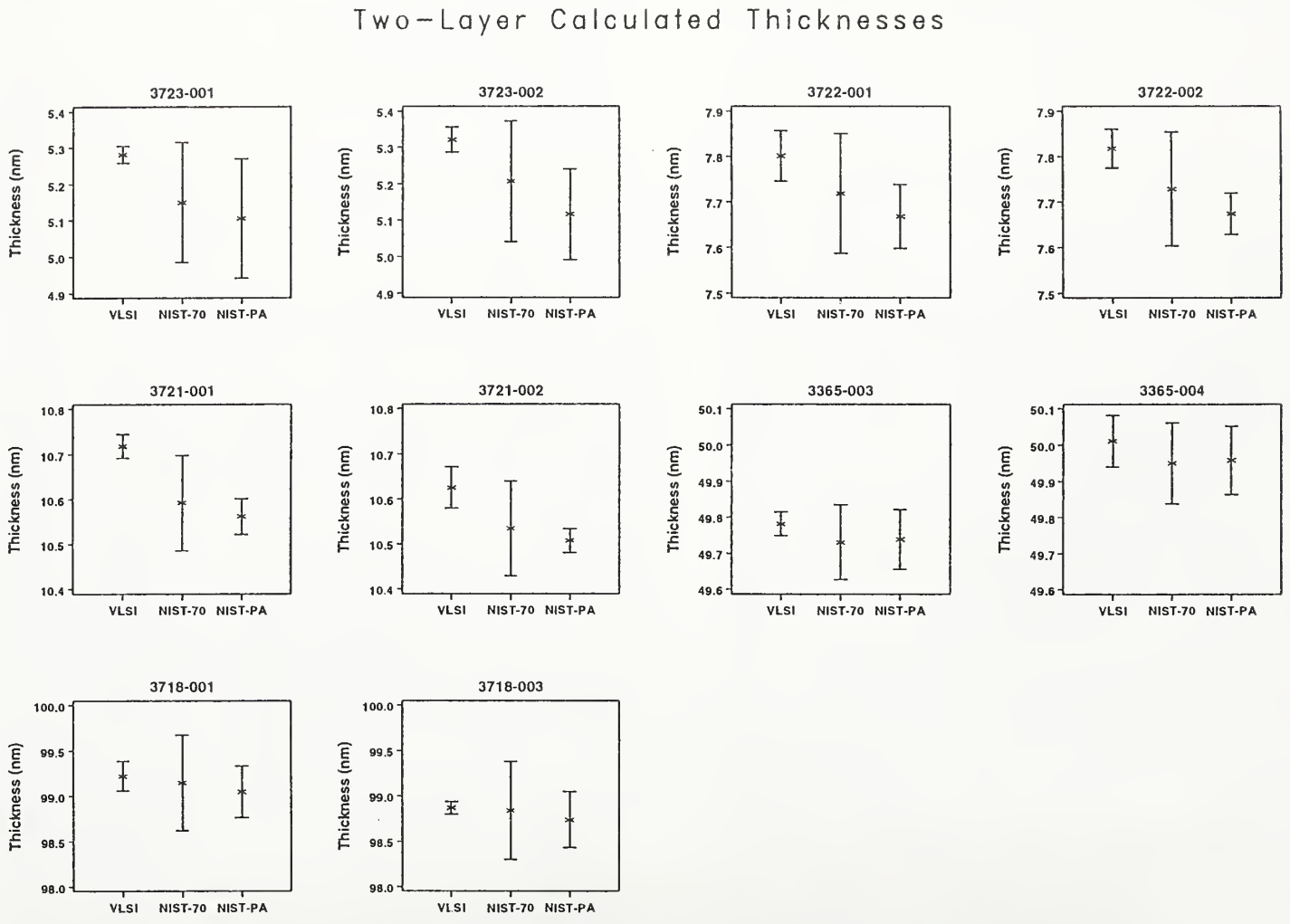

Figure 7. Comparison of calculated two-layer thickness values for three measurement methods: VLSI Standards at 70° angle of incidence, NIST at 70° angle of incidence, and NIST at the principal angle.

complexity of analyzing data from which film thickness values are calculated.

CONCLUSIONS

This CRADA was initiated to develop and test a two-laboratory measurement exchange procedure by which traceability to NIST could be demonstrated for single-wavelength ellipsometry measurements of thin oxide films that are outside the thickness range supported by NIST SRMs. In keeping with the needs of the semiconductor industry, as described in the *National Technical Roadmap for Semiconductors* (NTRS), the primary focus was to develop this capability in the <10 nm thickness regime; a very thick oxide was included in the testing, however, to support other applications. In addition, the two-laboratory measurement procedure itself was evaluated by NIST for effectiveness as a possible protocol for providing NIST Traceable Reference Materials (NTRMs) for future thin dielectric film standard artifacts, a logical extension of the NIST Standard Reference Materials Program.

Comparisons of ellipsometric measurements from another laboratory with those from the NIST High-Accuracy Ellipsometer are most directly made in terms of the ellipsometric parameters Δ and ψ. This gives a comparison of pure measurement equivalence without the added complexities introduced by the choice of a structural model to fit the data or choice of error function to be minimized during the fitting. CRADA measurements for the parameter Δ showed a small-to-moderate difference between the instruments at VLSI Standards and NIST, although the differences were statistically significant for only two of the 12 artifacts. The differences in Δ, as well as the associated expanded uncertainty values, were the largest for the 4.5 nm, 7.5 nm and 10 nm films. The increased differences for the thinnest films can be expected for several reasons: 1) Δ is a very sensitive function of change in film thickness due to contamination or atmospheric (moisture) variations (Fig. 2), or due to instrumental errors related to component alignment; and 2) there is a relatively greater difficulty in measuring these films with RAE ellipsometry since their values for Δ are quite large indicating polarization approaching linear, which is not an optimum measurement condition for photometric ellipsometry. An upper 95% Confidence Limit for the between-laboratory difference in values can be calculated from the difference in Δ values plus the expanded (2 σ) uncertainty of the difference. The two-sample average of this Confidence Limit is about 0.35° at 7.5 nm and about 0.60° at 4.5 nm; it is only about 0.17 at 1000 nm.

Differences found for ψ, although lower in magnitude than the differences in Δ, were statistically significant for nine of the 12 artifacts. However, for the three thinnest film categories, the calculated film thicknesses are almost entirely governed by the value of Δ. Therefore, differences found for ψ have little bearing on differences in calculated film thicknesses between the two laboratories.

Comparison of values of Δ and ψ is the most direct way to evaluate the accuracy of another laboratory's ellipsometer relative to the NIST instrument. However, acceptable values of the differences and uncertainties for these parameters are not intuitive, and the relation between Δ and ψ and calculated film thicknesses is nonlinear. Further, the customary user-desired output parameter for the ellipsometric measurement of a thin film is the thickness of the film. Comparisons of the calculated thickness values are therefore appropriate.

Using each laboratory's own algorithm and a single-layer model of the film gave average derived thickness values that were consistently within 0.1 nm of each other for all films in the first ellipsometric period at 70° (0 nm to 283 nm thick) except for the 50 nm films, and averaged just under 0.2 nm for the 1000 nm films. This result is generally satisfying since it represents less than a monolayer of SiO_2. By using the same algorithm (MAIN1) to process the data with a one-layer model (done for all but the 1000 nm films), the differences in the calculated thicknesses for the 50 nm samples were greatly reduced. These changes are believed to be due principally to the extent of the dependence of the calculated thickness of 50 nm films on both Δ and ψ and to the effect that the algorithms used by the two laboratories differ in the error functions upon which they minimize when determining thickness values that best fit the data.

Single-layer model thicknesses from the 70° data at both laboratories were generally well supported by comparison with the thicknesses from NIST principal angle measurements, with a lack of overlap of the 95% confidence intervals occurring in only one instance, that being the NIST 70° and principal angle data from one of the 10 nm films. This overall agreement is particularly satisfying because each of the methods of ellipsometry employed has different sensitivities and potential errors related to the optical components and the response of the photometer. Also, calculated thickness values from 70° and principal angle ellipsometry should only agree exactly if the model being used for the film/substrate system is known to be correct.

The assumption of using a fixed index of refraction relieves the large correlation of the index of refraction, n, and thickness, t, that occurs when solving the ellipsometric equations for very thin films. The precision in t, resulting from the fit to data, becomes very high, but the values for t suffer a loss of accuracy unless the chosen index value is known to be correct. Moreover, even if the index value is chosen correctly, accurately measured values of Δ and ψ cannot be fitted exactly to the single-layer model. This is because the evidence is that thermal oxides are nonideal, having an interface layer and strain that are not accounted for in the single-layer model. Simply put, failure to account for them in a single-layer model has a larger effect on the thickness calculated for the thinnest films. A single-layer model with agreed-upon optical index values was chosen for the principal comparison of the derived thicknesses in this study because of its simplicity.

The calculation of thicknesses from a two-layer model, while believed to be physically more correct and used for SRM certification, generally did not improve upon the single-layer comparison in this study. This may indicate that the assumption of a common interlayer thickness, to be extracted during simultaneous analysis of all artifacts, was not correct, perhaps due to the different lengths of time that were used for annealing the thick and thin films following oxide growth. In addition, NIST has had no prior experience including films <10 nm thick in the simultaneous fitting of a batch of samples to a two-layer model.

The best agreement in thickness values between the two laboratories results from the single-layer model. However, because of the limited number of sample exchanges, simple thickness differences are not the most appropriate expression of the results of the comparison. As noted in the case of the comparison for Δ, the Upper 95% Confidence Limit (absolute difference plus expanded uncertainty) for the between-laboratory differences is the preferred metric. For the 7.5 nm films, this Upper 95% Confidence Limit on thickness difference is between 0.11 nm and 0.14 nm, depending on whether

individual algorithms, or a common algorithm, is used. For the 4.5 nm films, this Confidence Limit increases to about 0.20 nm or 0.23 nm, again depending on algorithm used. For the 1000 nm films, this Confidence Limit has an average value of 0.32 nm for the case of individual algorithms. Since the expanded uncertainties are larger than the calculated average differences for these two films, it is not statistically meaningful to use the calculated differences as scale offsets for VLSI Standards' results with respect to NIST.

Both laboratories have long-term experience measuring artifacts in the 10 nm to 100 nm range, hence the artifacts in this range served as a baseline for this study. A few simple conclusions can be drawn from the results for these artifacts: 1) there are measurable, but generally statistically insignificant, differences in Δ values between the labs; 2) these offsets vs. thickness follow a pattern that suggests a specific mechanism to be the cause, but no clear explanation was found; 3) the differences in ψ values were smaller, but generally statistically significant, and relatively independent of thickness; 4) there is a very minor algorithm dependence ($\leq$0.05 nm) of the thickness for the 10 nm and 100 nm films, but a more noticeable (~ 0.23 nm) for the 50 nm films; 5) simple thickness differences following common-algorithm analysis appear acceptably small with no patterns detectable and only one difference value that is statistically significant; and 6) expanded uncertainty values show room for improvement of both the "within-laboratory" and "between-laboratory" components in future testing of this type.

The differences and variations that were obtained in this study do not appear unreasonable considering the 6-month duration, eight transcontinental shipments and lack of single-laboratory environment control, as well as totally different types of instruments. In studying the data from the experiment, certain unresolved ambiguities were observed. The possibility of such ambiguities was the reason multiple artifact exchanges were required in order to better estimate the realistic uncertainty of the laboratory measurement exchange process. The study was planned for four to six artifact exchanges, but only four were completed during the 6-month period. There were occasions where the respective measurement systems may not have been in statistical control, as noted in Appendix 2, and there was some evidence of artifact drift seen in the NIST 70° data for the 4.5 nm and 7.5 nm films, although this was not supported by the other measurements on the artifacts. In future measurement exchanges of this type, the design should require six or more exchanges, which would allow the possibility of data screening. Also, the current study was not optimized to detect artifact instability. The use of control chart measurements made in coordination with the intercomparison measurements, but on additional sets of artifacts retained by the individual laboratories, should be added to any future studies.

In summary, the two-laboratory agreement for the 7.5 nm oxide films, as measured by the 95% Upper Confidence Limits for the difference, is well within the NTRS manufacturing tolerance interval for films at this thickness but not within the stringent precision-to-tolerance ratio for instrumentation used for monitoring the production processes for these films.. In the case of the 4.5 nm films, the 95% Upper Confidence Limit for the two-laboratory thickness difference is actually slightly larger than the NTRS manufacturing tolerance interval. This indicates very clearly that additional work is needed in order to tighten the agreement to levels commensurate with the needs of the semiconductor industry as stated in the NTRS.

REFERENCES

[1] The National Technology Roadmap for Semiconductors, Semiconductor Industry Association, 1997, San Jose, CA.

[2] G. A. Candela, D. Chandler-Horowitz, J. F. Marchiando, D. B. Novotny, B. J. Belzer, and M. C. Croarkin, *Standard Reference Materials*: Preparation and Certification of SRM-2530, Ellipsometric Parameters Δ and ψ and Derived Thickness and Refractive Index of a Silicon Dioxide Layer on Silicon, NIST Special Publication 260-109 (October 1988).

[3] D. Chandler-Horowitz and G. A. Candela, An Ellipsometry System for High Accuracy Metrology of Thin Films, SPIE **480**, Integrated Circuit Metrology II, 2-8 (1984).

[4] N. V. Nguyen and C. A. Richter, Thickness Determination of Ultra-Thin SiO_2 Films on Si by Spectroscopic Ellipsometry, in *Silicon Nitride and Silicon Dioxide Thin Insulating Films,* Proceedings of the Conference, Vol. 97-10, M. J. Deen, W. D. Brown, K. B. Sundaram, and S. I. Raider, Eds. (The Electrochemical Society, Inc., Pennington, New Jersey), pp 183-193.

[5] G. E. Jellison, Jr., The Calculation of Thin Film Parameters from Spectroscopic Ellipsometry Data, Thin Solid Films 290-291, 40-45 (1996).

[6] J. Geist, A. R. Schaefer, J-F Song, Y. H. Wang, and E. F. Zalewski, An Accurate Value for the Absorption Coefficient of Silicon at 633 nm, J. Res. Natl. Inst. Stand. Technol. **95**, 549 (1990).

[7] J. M. Marchiando, *Semiconductor Measurement Technology*: A Software Program for Aiding the Analysis of Ellipsometric Measurements, Simple Models, NIST Special Publication 400-83 (July 1989).

[8] B. J. Belzer and D. L. Blackburn, *Semiconductor Measurement Technology*: The Results of an Interlaboratory Study of Ellipsometric Measurements of Thin Silicon Dioxide on Silicon, NIST Special Publication 400-99 (May 1997).

[9] There are currently conflicting sources for the optical constants of the silicon substrate used in modeling the spectroscopic ellipsometry data. Until such time as a set of values is agreed upon by the metrology community at large, between-laboratory comparisons of data obtained by using spectroscopic ellipsometry have limited usefulness.

[10] E. D. Palik, ed., Handbook of Optical Constants of Solids, Academic Press Inc., New York, 719-763 (1985).

[11] D. Chandler-Horowitz and G. A. Candela, Principal Angle Spectroscopic Ellipsometry Utilizing a Rotating Analyzer, Applied Optics **21**, 2971-2977 (15 August 1982).

[12] R. M. A. Azzam and N. M. Bashara, Ellipsometry and Polarized Light, paperback edition (North-Holland Amsterdam, 1987).

[13] R. W. Collins, Automatic Rotating Element Ellipsometers: Calibration, Operation, and Real-time Applications, Rev. Sci. Instrum, **61** (8), 2029-2062 (August 1990).

[14] C. P. Reeve, The Calibration of Indexing Tables by Subdivision, NBSIR 75-750 (July 1975).

APPENDIX 1. CALCULATION OF EXPANDED UNCERTAINTIES

The expanded uncertainties in Tables 2 to 6 were calculated using the ISO method [A1.1]. In this case, the resulting expanded uncertainty coincides with a 95% statistical confidence interval for the difference of the two means. The method of calculation is described as follows.

For each measurement method, NIST PA, NIST 70°, and VLSI Standards 70°, there were 20 measurements made on each artifact during the four exchanges, five measurements per exchange. These 20 measurements were first reduced to the mean value per exchange, resulting in four mean values. Next, the resulting four mean values were summarized by computing their mean and standard deviation. For method i, let $\bar{x}_i$ denote the resulting mean value and let s_i denote the corresponding standard deviation. Note that s_i has degrees of freedom equal to three since it is calculated from the deviations among four summary values. Also note that the quantity $\bar{x}_i$ is equal to the grand mean of the 20 measurements, since the number of measurements per exchange was constant (and equal to five).

The tabulated difference between two measurement methods, say i and j, is then given as $(\bar{x}_i - \bar{x}_j)$, and the expanded uncertainty is calculated as $U = ku_c$, where

$$u_c = \sqrt{\left(\frac{s_i}{\sqrt{4}}\right)^2 + \left(\frac{s_j}{\sqrt{4}}\right)^2},$$

and where k is a factor from the Student-t distribution for 95% confidence and degrees of freedom ν_{eff} given by the Satterthwaite formula [A1.1, p. 64],

$$\nu_{eff} = \frac{u_c^4}{\frac{\left(s_1/\sqrt{4}\right)^4}{3} + \frac{\left(s_2/\sqrt{4}\right)^4}{3}}.$$

REFERENCE

[A1.1] *Guide to the Expression of Uncertainty in Measurement*, ISBN 92-67-10188-9, 1st Ed. ISO, Geneva, Switzerland (1993). See also Taylor, B. N. and Kuyatt, C. E., Guidelines for Evaluating and Expressing the Uncertainty of NIST Measurement Results, NIST Technical Note 1297, U.S. Government Printing Office, Washington, DC. (1994).

Appendix 2. Between- and Within-Exchange Variation in Ellipsometry Measurements

In the experiment design for this interlaboratory comparison, four exchanges of the artifacts and five independent measurements per exchange were made on each artifact. It was decided to exchange the artifacts several times over a period of months based on the common experience that laboratory measurement processes tend to exhibit greater variation over long time periods than will be seen during a shorter period of a few days. That this proved true can be seen in the accompanying Figures A2.1 to A2.4. In these figures, the Δ and ψ values from the NIST and VLSI Standards measurement processes are plotted, for each artifact, against the time index 1 to 4, corresponding to the four artifact exchanges during the intercomparison.

For many of the measurement series associated with various artifacts, the shifts in the mean level of the measurements that are visible to the eye can be shown to be statistically significant differences by a formal statistical analysis of variance (ANOVA) procedure. The details of exactly which measurement series show statistically significant differences between artifact exchanges is not so important once it is accepted that the measurement processes involved have the tendency to exhibit greater variability over long time periods than short time periods. It is important that any uncertainty analysis used should properly account for this behavior. The uncertainty analysis procedure described in Appendix 1 was designed to ensure that both the long-range and short-range variability of the NIST and VLSI Standards measurement processes are properly represented in the uncertainty analyses presented in this report.

Study of the plots in Figures A2.1 to A2.4 shows that the NIST data for exchange 1 (July 1996) and the VLSI Standards data for exchange 4 (December 1996) are somewhat anomalous, compared to the other data. In the NIST data for exchange 1, and for the three thinnest films, the values of Δ tend to be high relative to the other exchanges, while those for ψ tend to be relatively low. In the VLSI Standards data for exchange 4, the variability of both the Δ and ψ data is noticeably larger than for the other time periods. These observations suggest that the measurement systems may not have in strict statistical control during those respective time periods.

The statistical design for this intercomparison included a provision for continuing without modification the maintenance of control charts on the measurement systems at the two laboratories. In both cases, this meant remeasuring NIST-certified thin film standards at regular intervals, which turned out to be about once a month at VLSI Standards and about twice a month at NIST. However, the schedule of control chart measurements was not specifically coordinated with the intercomparison measurements in either laboratory, and the control chart measurements would not have been effective for signaling out-of-control conditions that would affect the intercomparison measurements.

A lesson learned from this experience, which should be applied in future comparisons of this type, is that it would be better to design the study in a way that ensures that at least some relevant control chart measurements (using artifacts in or near the size range of the intercomparison artifacts) should be made in coordination (e.g., same day) with the intercomparison measurements. This would allow the control chart measurements to be used to diagnose out-of-

control conditions in the measurement systems so that such conditions could be corrected before the measurements are completed. This would likely have the effect of lowering the uncertainty and increasing the quality of the results of the comparison.

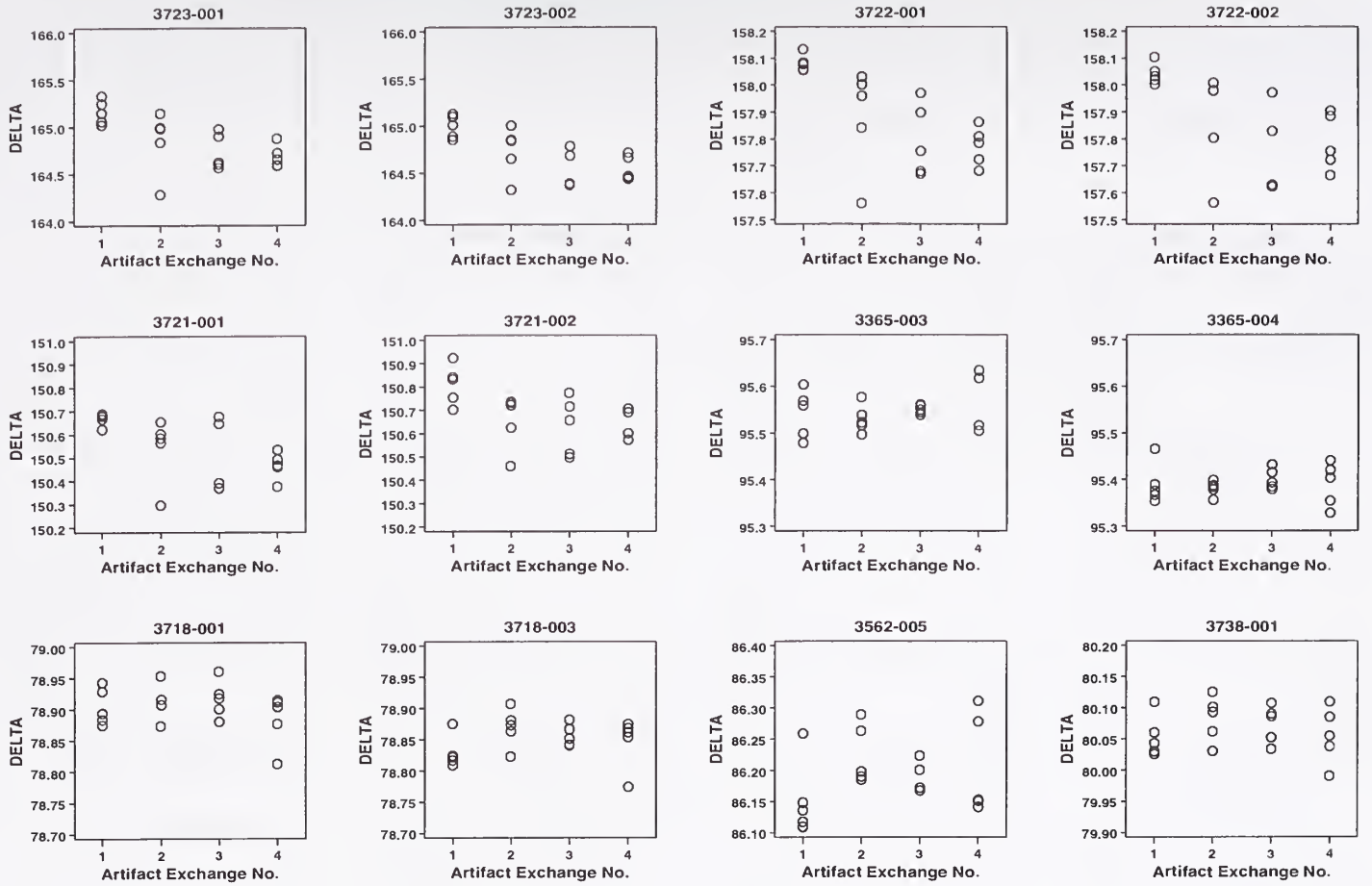

Figure A2.1 – NIST 70° data. Plots of Δ versus a time index corresponding to the four artifact exchanges in the interlaboratory comparison. The data are from the NIST 70° measurements, plotted separately for each of the 12 artifacts. The plots show the tendency for the measurement process to undergo significant variation over longer time periods (between exchanges) that exceeds the short-term variability seen within exchanges.

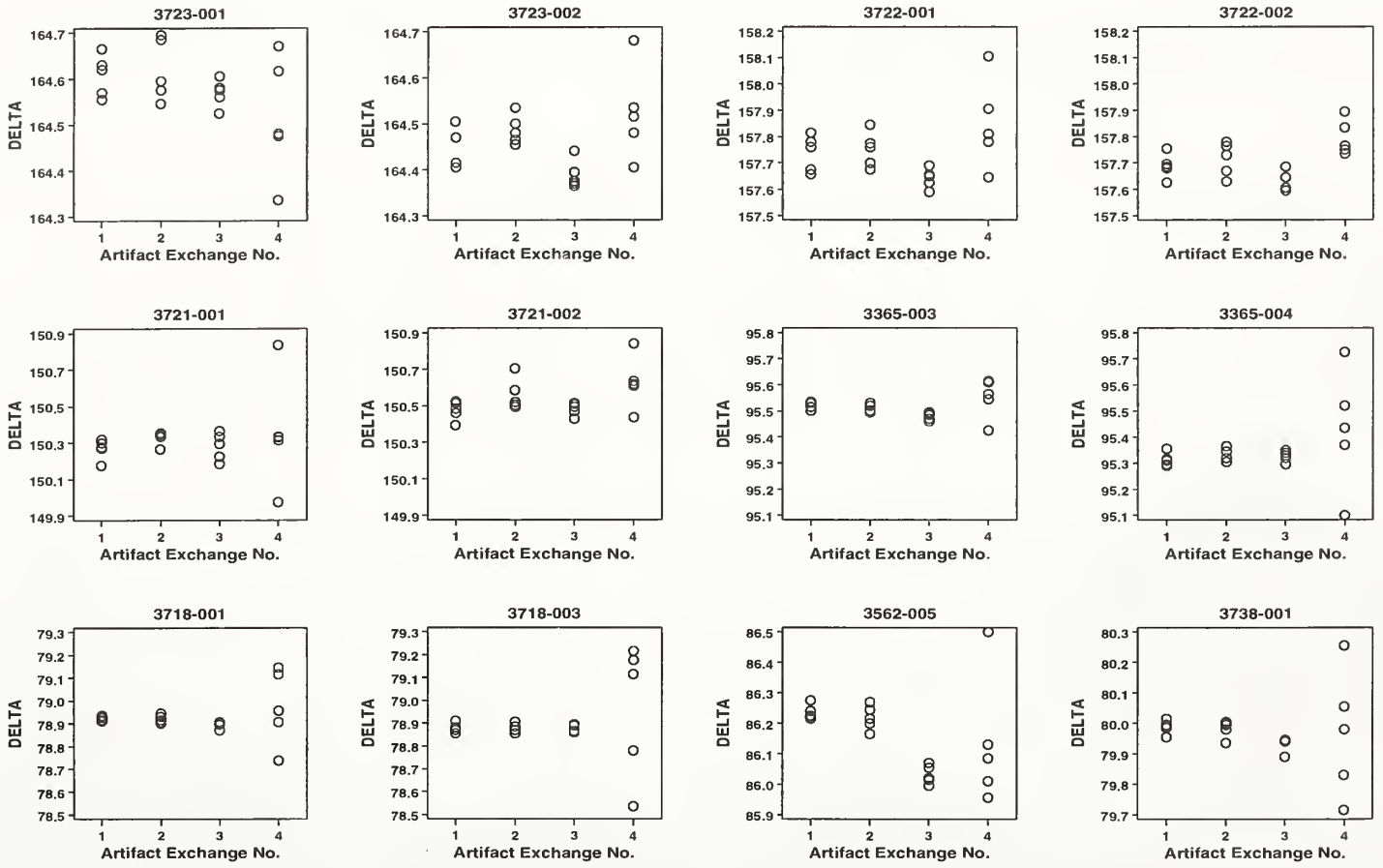

Figure A2.2 – VLSI Standards data. Plots of Δ versus a time index corresponding to the four artifact exchanges in the interlaboratory comparison. The data are from the VLSI 70° measurements, plotted separately for each of the 12 artifacts. The plots show the tendency for the measurement process to undergo significant variation over longer time periods (between exchanges) that exceeds the short-term variability seen within exchanges.

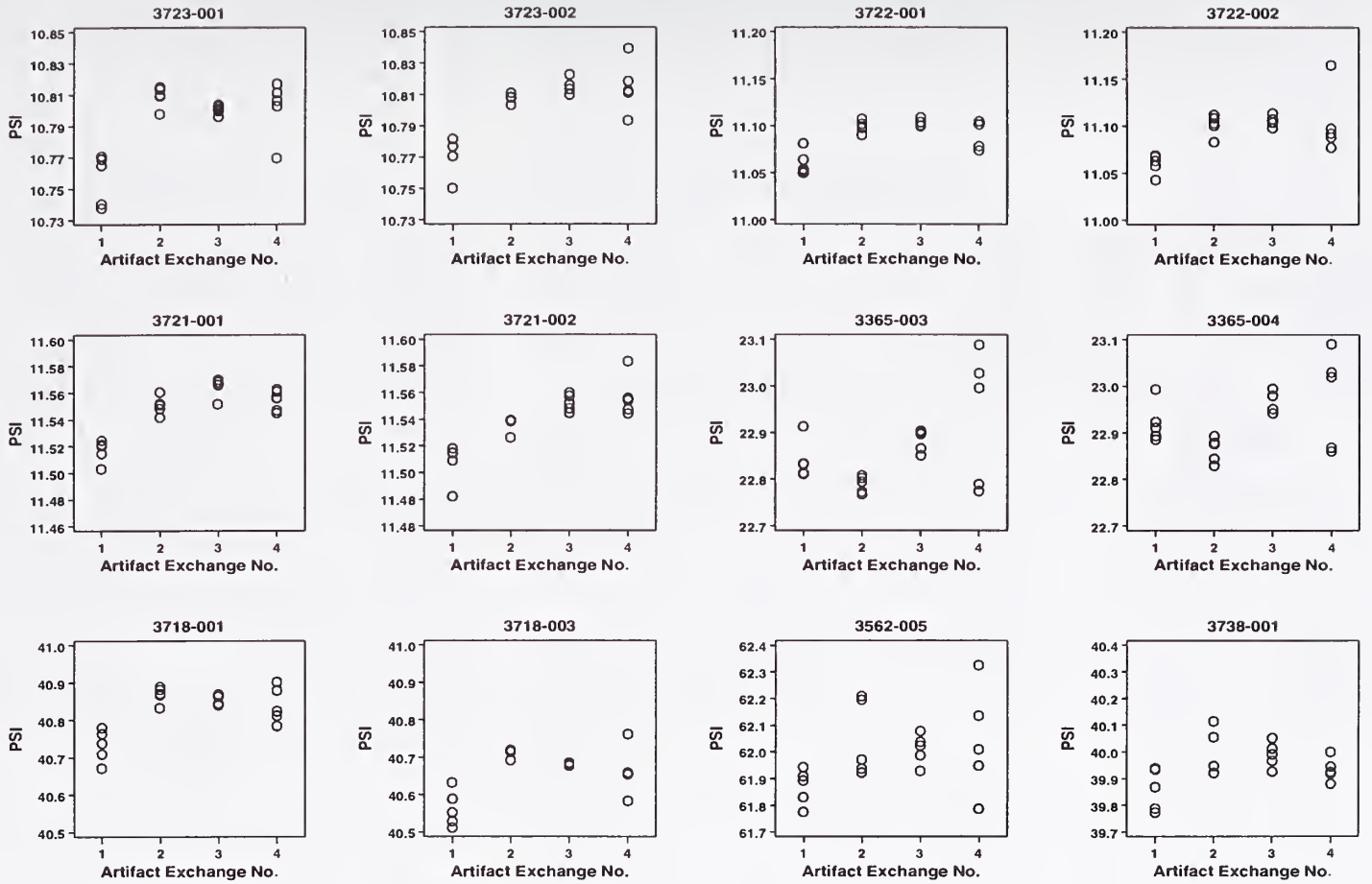

Figure A2.3 – NIST 70° data. Plots of ψ versus a time index corresponding to the four artifact exchanges in the interlaboratory comparison. The data are from the NIST 70° measurements, plotted separately for each of the 12 artifacts. The plots show the tendency for the measurement process to undergo significant variation over longer time periods (between exchanges) that exceeds the short-term variability seen within exchanges.

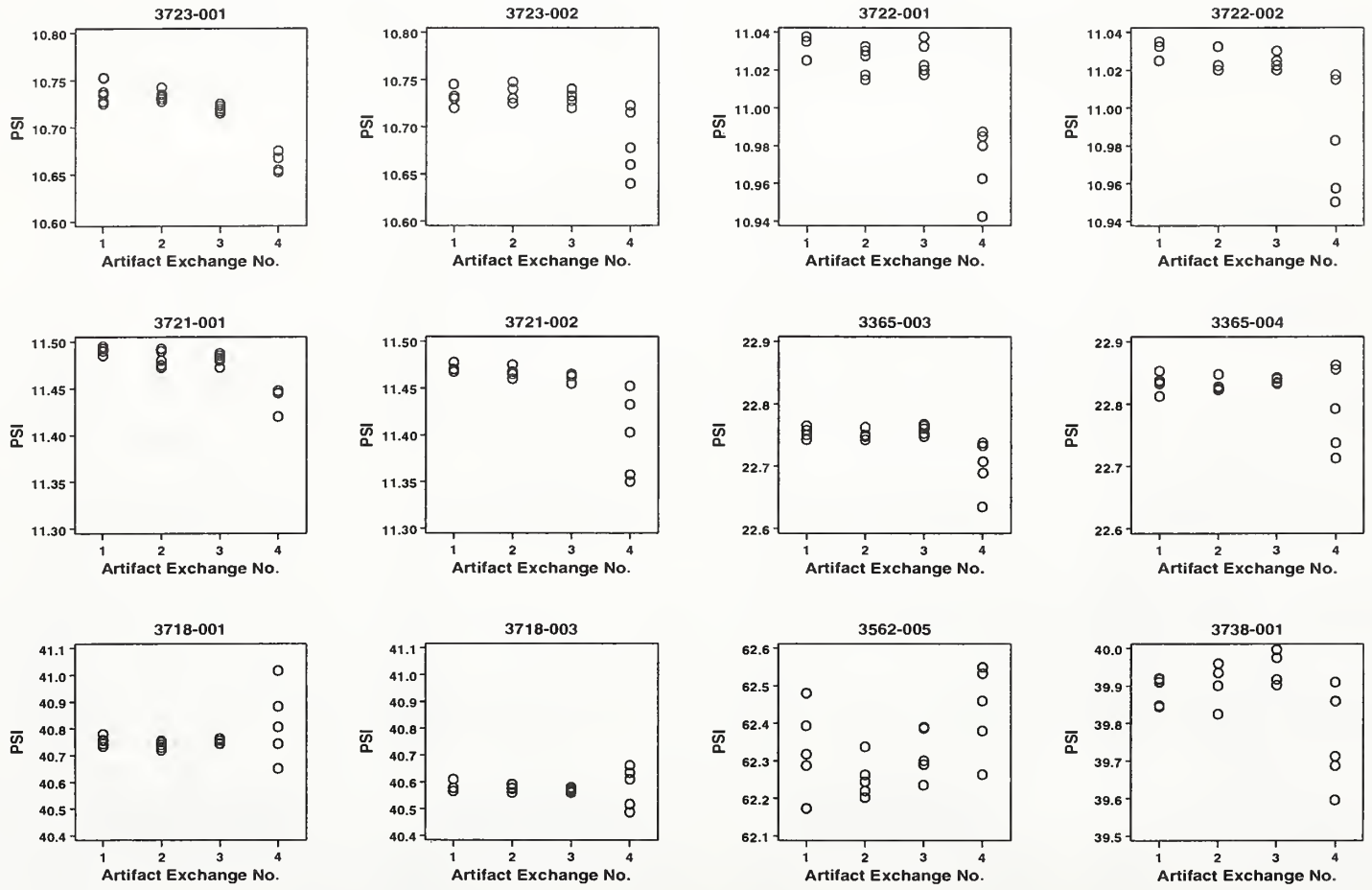

Figure A2.4 – VLSI Standards data. Plots of ψ versus a time index corresponding to the four artifact exchanges in the interlaboratory comparison. The data are from the VLSI Standards 70° measurements, plotted separately for each of the 12 artifacts. The plots show the tendency for the measurement process to undergo significant variation over longer time periods (between exchanges) that exceeds the short-term variability seen within exchanges.

APPENDIX 3. THICKNESS VALUES USING REGRESSION TECHNIQUE FOR SiO_2 FILM ON SILICON SUBSTRATE

Spectroscopic ellipsometer results:
Wavelength range: 300 to 800 nm Number of spectral points: 120
Beam size: 2 x 8 mm
Angle of incidence: (74.98 + 0.01) degrees
Refractive index used in modeling: Handbook of Optical Constants of Solids, E. D. Palik

RUN # 1

	Thickness in nanometers using Regression technique							
Serial No.	center	top	bottom	left	right	average	nonuniformity	std. dev.
3723-001	4.38	4.42	4.49	4.48	4.54	4.462	0.16	0.06
3723-002	4.54	4.56	4.58	4.49	4.44	4.522	0.14	0.06
3722-001	6.95	6.91	6.84	7.00	6.97	6.934	0.16	0.06
3722-002	6.86	6.92	6.97	7.00	7.01	6.952	0.15	0.06
3721-001	9.92	9.93	9.95	9.91	10.04	9.95	0.13	0.05
3721-002	9.92	9.93	9.94	9.88	9.92	9.918	0.06	0.02
3365-003	49.72	49.68	49.74	49.75	49.70	49.718	0.07	0.03
3365-004	50.04	50.09	49.98	50.00	50.07	50.036	0.11	0.05
3718-001	98.58	98.54	98.66	98.52	98.79	98.618	0.27	0.11
3718-003	98.38	98.34	98.50	98.27	98.34	98.366	0.23	0.08
3562-005	1009.21	1008.33	1008.59	1008.79	1008.67	1008.718	0.88	0.32
3738-001	1034.51	1034.58	1036.04	1034.72	1035.53	1035.076	1.53	0.68

RUN # 2

	Thickness in nanometers using Regression technique							
Serial No.	center	top	bottom	left	right	average	nonuniformity	std. dev.
3723-001	4.59	4.59	4.60	4.57	4.63	4.596	0.06	0.02
3723-002	4.63	4.67	4.65	4.61	4.69	4.65	0.08	0.03
3722-001	7.10	7.13	7. 14	7.16	7.13	7.13	0.06	0.02
3722-002	7.11	7.16	7.14	7.13	7.06	7.12	0.1	0.04
3721-001	10.08	10.05	10.01	10.02	10.10	10.052	0.09	0.04
3721-002	9.96	9.98	9.99	9.99	10.07	9.998	0.11	0.04
3365-003	49.76	49.75	49.82	49.81	49.76	49.78	0.07	0.03
3365-004	50.08	50.13	50.04	50.06	50.13	50.088	0.09	0.04
3718-001	98.75	98.71	98.93	98.73	98.97	98.8182	0.259	0.12
3718-003	98.56	98.50	98.54	98.50	98.68	98.556	0.18	0.07
3562-005	1008.48	1008.25	1009.24	1008.76	1008.24	1008.594	1	0.42
3738-001	1036.65	1036.91	1037.23	1036.31	1037.35	1036.89	1.04	0.42

Table A2.1 NIST 70° Data

		Δ		ψ		One-Layer Thickness		Two-Layer Thickness	
Sample	Date	Mean	Std Dev	Mean	Std Dev	Mean	Std Dev	Mean	Std Dev
3723-001	Jul-96	165.161	0.128	10.757	0.016	4.994	0.046	4.999	0.046
3723-001	Sep-96	164.848	0.334	10.809	0.007	5.108	0.118	5.166	0.120
3723-001	Oct-96	164.732	0.190	10.801	0.003	5.145	0.066	5.207	0.069
3723-001	Dec-96	164.684	0.117	10.801	0.019	5.166	0.042	5.228	0.042
3723-002	Jul-96	164.996	0.123	10.766	0.015	5.053	0.043	5.058	0.044
3723-002	Sep-96	164.733	0.264	10.808	0.003	5.148	0.093	5.207	0.095
3723-002	Oct-96	164.523	0.195	10.814	0.005	5.218	0.068	5.282	0.070
3723-002	Dec-96	164.544	0.132	10.815	0.017	5.216	0.047	5.278	0.047
3722-001	Jul-96	158.087	0.028	11.060	0.013	7.613	0.010	7.598	0.010
3722-001	Sep-96	157.879	0.192	11.099	0.006	7.693	0.073	7.735	0.073
3722-001	Oct-96	157.794	0.134	11.103	0.004	7.725	0.051	7.766	0.051
3722-001	Dec-96	157.772	0.071	11.092	0.014	7.733	0.027	7.777	0.027
3722-002	Jul-96	158.042	0.039	11.060	0.011	7.630	0.015	7.615	0.015
3722-002	Sep-96	157.866	0.188	11.101	0.011	7.698	0.071	7.739	0.071
3722-002	Oct-96	157.735	0.158	11.105	0.006	7.747	0.060	7.788	0.060
3722-002	Dec-96	157.786	0.105	11.104	0.035	7.728	0.039	7.772	0.039
3721-001	Jul-96	150.667	0.026	11.517	0.009	10.530	0.011	10.494	0.011
3721-001	Sep-96	150.540	0.140	11.551	0.007	10.582	0.057	10.606	0.056
3721-001	Oct-96	150.490	0.156	11.564	0.007	10.603	0.064	10.627	0.063
3721-001	Dec-96	150.465	0.057	11.554	0.008	10.613	0.023	10.639	0.023
3721-002	Jul-96	150.811	0.085	11.508	0.015	10.471	0.035	10.436	0.034
3721-002	Sep-96	150.654	0.118	11.536	0.006	10.536	0.048	10.560	0.048
3721-002	Oct-96	150.631	0.122	11.552	0.006	10.546	0.050	10.570	0.050
3721-002	Dec-96	150.628	0.065	11.557	0.015	10.547	0.026	10.574	0.026
3365-003	Jul-96	95.541	0.052	22.840	0.042	50.110	0.045	49.635	0.044
3365-003	Sep-96	95.530	0.030	22.789	0.018	50.098	0.028	49.746	0.028
3365-003	Oct-96	95.550	0.009	22.883	0.023	50.122	0.019	49.779	0.019
3365-003	Dec-96	95.578	0.062	22.935	0.143	50.116	0.012	49.763	0.012
3365-004	Jul-96	95.390	0.044	22.921	0.043	50.328	0.033	49.849	0.033
3365-004	Sep-96	95.381	0.016	22.864	0.026	50.310	0.010	49.955	0.010
3365-004	Oct-96	95.401	0.022	22.969	0.022	50.340	0.037	49.994	0.036
3365-004	Dec-96	95.389	0.046	22.973	0.104	50.356	0.015	50.000	0.014
3718-001	Jul-96	78.905	0.030	40.733	0.043	99.090	0.078	98.653	0.080
3718-001	Sep-96	78.913	0.029	40.868	0.022	99.335	0.038	99.332	0.039
3718-001	Oct-96	78.917	0.030	40.852	0.013	99.306	0.020	99.319	0.021
3718-001	Dec-96	78.884	0.043	40.840	0.049	99.280	0.083	99.284	0.087
3718-003	Jul-96	78.830	0.027	40.563	0.049	98.783	0.083	98.331	0.090
3718-003	Sep-96	78.870	0.031	40.711	0.011	99.047	0.020	99.037	0.021
3718-003	Oct-96	78.857	0.018	40.682	0.003	98.991	0.007	98.998	0.007
3718-003	Dec-96	78.847	0.041	40.684	0.077	98.994	0.137	98.991	0.142
3562-005	Jul-96	86.154	0.061	61.870	0.067	1008.186	0.038		
3562-005	Sep-96	86.225	0.048	62.046	0.143	1008.049	0.108		
3562-005	Oct-96	86.193	0.023	62.010	0.056	1008.081	0.036		
3562-005	Dec-96	86.207	0.081	62.041	0.202	1008.057	0.141		
3738-001	Jul-96	80.054	0.034	39.860	0.078	1034.843	0.157		
3738-001	Sep-96	80.082	0.037	39.992	0.088	1034.578	0.174		
3738-001	Oct-96	80.074	0.030	39.989	0.047	1034.583	0.093		
3738-001	Dec-96	80.056	0.046	39.933	0.043	1034.695	0.088		

Table A2.2 VLSI Standards, Inc. 70° Data

		Δ		Ψ		One-Layer Thick (VLSI)		One-Layer Thick (Main1)		Two-Layer Thickness	
Sample	Date	Mean	Std Dev	Mean	Std Dev	Mean	Std Dev	Mean	Std Dev	Mean	Std Dev
3723-001	Jun-96	164.608	0.045	10.736	0.011	5.181	0.018	5.193	0.016	5.270	0.016
3723-001	Aug-96	164.619	0.067	10.734	0.006	5.177	0.025	5.183	0.023	5.269	0.027
3723-001	Oct-96	164.569	0.029	10.720	0.004	5.189	0.009	5.207	0.010	5.284	0.011
3723-001	Dec-96	164.515	0.132	10.664	0.009	5.188	0.045	5.225	0.047	5.301	0.047
3723-002	Jun-96	164.460	0.048	10.732	0.009	5.231	0.016	5.246	0.017	5.324	0.017
3723-002	Aug-96	164.487	0.032	10.737	0.009	5.224	0.013	5.229	0.011	5.314	0.012
3723-002	Oct-96	164.389	0.031	10.730	0.007	5.256	0.012	5.271	0.011	5.349	0.011
3723-002	Dec-96	164.523	0.101	10.683	0.035	5.192	0.040	5.223	0.036	5.298	0.036
3722-001	Jun-96	157.737	0.069	11.032	0.006	7.723	0.024	7.745	0.026	7.806	0.026
3722-001	Aug-96	157.751	0.067	11.025	0.008	7.715	0.027	7.740	0.025	7.800	0.025
3722-001	Oct-96	157.642	0.037	11.026	0.009	7.754	0.017	7.781	0.014	7.841	0.014
3722-001	Dec-96	157.849	0.171	10.972	0.019	7.653	0.069	7.702	0.065	7.756	0.063
3722-002	Jun-96	157.688	0.046	11.032	0.004	7.740	0.015	7.764	0.018	7.825	0.017
3722-002	Aug-96	157.715	0.064	11.026	0.006	7.728	0.023	7.753	0.024	7.814	0.024
3722-002	Oct-96	157.625	0.039	11.025	0.004	7.759	0.015	7.788	0.015	7.848	0.015
3722-002	Dec-96	157.796	0.067	10.985	0.031	7.678	0.019	7.722	0.025	7.783	0.025
3721-001	Jun-96	150.268	0.056	11.491	0.004	10.657	0.021	10.691	0.023	10.735	0.023
3721-001	Aug-96	150.331	0.038	11.482	0.009	10.629	0.018	10.665	0.016	10.709	0.015
3721-001	Oct-96	150.281	0.075	11.482	0.006	10.646	0.029	10.686	0.031	10.728	0.031
3721-001	Dec-96	150.358	0.307	11.436	0.015	10.588	0.110	10.653	0.125	10.699	0.124
3721-002	Jun-96	150.476	0.052	11.471	0.004	10.569	0.020	10.606	0.021	10.650	0.021
3721-002	Aug-96	150.562	0.087	11.467	0.005	10.536	0.034	10.571	0.036	10.615	0.035
3721-002	Oct-96	150.484	0.035	11.463	0.004	10.561	0.014	10.603	0.014	10.645	0.014
3721-002	Dec-96	150.628	0.144	11.399	0.045	10.466	0.049	10.542	0.058	10.589	0.058
3365-003	Jun-96	95.516	0.016	22.753	0.009	49.879	0.022	50.096	0.021	49.777	0.021
3365-003	Aug-96	95.508	0.016	22.750	0.007	49.878	0.021	50.103	0.021	49.781	0.021
3365-003	Oct-96	95.480	0.015	22.759	0.008	49.909	0.023	50.140	0.021	49.811	0.021
3365-003	Dec-96	95.552	0.077	22.701	0.041	49.759	0.110	50.027	0.104	49.761	0.103
3365-004	Jun-96	95.313	0.026	22.834	0.014	50.149	0.041	50.374	0.036	50.051	0.035
3365-004	Aug-96	95.336	0.024	22.830	0.010	50.125	0.022	50.345	0.028	50.019	0.027
3365-004	Oct-96	95.327	0.021	22.838	0.004	50.145	0.012	50.359	0.024	50.027	0.024
3365-004	Dec-96	95.430	0.228	22.792	0.068	50.000	0.127	50.216	0.251	49.947	0.249
3718-001	Jun-96	78.923	0.010	40.754	0.018	99.172	0.033	99.130	0.032	99.186	0.033
3718-001	Aug-96	78.919	0.019	40.739	0.014	99.145	0.026	99.103	0.025	99.152	0.026
3718-001	Oct-96	78.895	0.015	40.752	0.008	99.168	0.015	99.123	0.015	99.171	0.015
3718-001	Dec-96	78.971	0.167	40.820	0.140	99.294	0.260	99.255	0.264	99.372	0.268
3718-003	Jun-96	78.879	0.020	40.586	0.023	98.858	0.043	98.821	0.043	98.869	0.044
3718-003	Aug-96	78.877	0.019	40.579	0.013	98.846	0.025	98.814	0.025	98.849	0.026
3718-003	Oct-96	78.881	0.017	40.571	0.008	98.830	0.015	98.794	0.015	98.831	0.015
3718-003	Dec-96	78.964	0.295	40.583	0.076	98.854	0.143	98.825	0.142	98.930	0.146
3562-005	Jun-96	86.235	0.024	62.330	0.115	1007.893	0.087				
3562-005	Aug-96	86.219	0.041	62.254	0.052	1007.951	0.041				
3562-005	Oct-96	86.031	0.031	62.321	0.067	1007.911	0.050				
3562-005	Dec-96	86.136	0.214	62.437	0.118	1007.818	0.096				
3738-001	Jun-96	79.988	0.022	39.888	0.038	1034.807	0.073				
3738-001	Aug-96	79.983	0.028	39.916	0.057	1034.749	0.111				
3738-001	Oct-96	79.932	0.024	39.942	0.042	1034.700	0.082				
3738-001	Dec-96	79.967	0.208	39.754	0.129	1035.070	0.254				

Table A2.3 NIST Principal Angle Data

		Δ		ψ		One-Layer Thickness		Two-Layer Thickness	
Sample	Date	Mean	Std Dev	Mean	Std Dev	Mean	Std Dev	Mean	Std Dev
3723-001	Jul-96	89.763	0.372	3.018	0.015	5.210	0.279	5.092	0.285
3723-001	Sep-96	89.805	0.152	3.011	0.011	5.175	0.111	5.052	0.116
3723-001	Oct-96	89.675	0.079	3.013	0.010	5.274	0.062	5.255	0.064
3723-001	Dec-96	89.845	0.087	3.018	0.023	5.149	0.069	5.024	0.072
3723-002	Jul-96	90.040	0.448	3.045	0.017	5.171	0.326	5.056	0.334
3723-002	Sep-96	90.004	0.042	3.038	0.014	5.193	0.029	5.074	0.030
3723-002	Oct-96	89.937	0.106	3.053	0.012	5.250	0.075	5.229	0.078
3723-002	Dec-96	89.971	0.216	3.053	0.019	5.222	0.160	5.105	0.167
3722-001	Jul-96	89.971	0.254	4.407	0.018	7.716	0.197	7.607	0.196
3722-001	Sep-96	89.885	0.033	4.413	0.014	7.782	0.030	7.670	0.030
3722-001	Oct-96	89.935	0.026	4.415	0.009	7.748	0.024	7.685	0.021
3722-001	Dec-96	89.837	0.085	4.412	0.017	7.819	0.068	7.711	0.062
3722-002	Jul-96	89.926	0.242	4.416	0.020	7.753	0.189	7.644	0.189
3722-002	Sep-96	89.884	0.020	4.415	0.015	7.784	0.021	7.672	0.021
3722-002	Oct-96	89.903	0.013	4.424	0.010	7.773	0.012	7.713	0.012
3722-002	Dec-96	89.888	0.240	4.416	0.014	7.782	0.180	7.670	0.180
3721-001	Jul-96	89.930	0.200	5.958	0.020	10.642	0.160	10.533	0.159
3721-001	Sep-96	89.900	0.030	5.958	0.010	10.665	0.023	10.554	0.023
3721-001	Oct-96	89.914	0.107	5.971	0.016	10.659	0.085	10.568	0.084
3721-001	Dec-96	89.856	0.047	5.972	0.012	10.704	0.038	10.592	0.038
3721-002	Jul-96	89.764	0.267	5.931	0.018	10.597	0.211	10.487	0.211
3721-002	Sep-96	89.727	0.053	5.924	0.011	10.622	0.042	10.510	0.042
3721-002	Oct-96	89.742	0.033	5.942	0.015	10.618	0.030	10.527	0.030
3721-002	Dec-96	89.738	0.102	5.941	0.007	10.620	0.081	10.507	0.081
3365-003	Jul-96	89.938	0.066	22.789	0.044	50.144	0.057	49.777	0.057
3365-003	Sep-96	89.938	0.022	22.733	0.022	50.110	0.023	49.740	0.023
3365-003	Oct-96	89.946	0.010	22.833	0.025	50.162	0.012	49.665	0.012
3365-003	Dec-96	89.973	0.071	22.879	0.122	50.156	0.029	49.774	0.029
3365-004	Jul-96	89.938	0.047	22.875	0.045	50.381	0.037	50.011	0.037
3365-004	Sep-96	89.955	0.023	22.812	0.025	50.321	0.031	49.949	0.030
3365-004	Oct-96	89.962	0.026	22.920	0.015	50.379	0.040	49.878	0.040
3365-004	Dec-96	89.964	0.054	22.922	0.098	50.378	0.009	49.994	0.009
3718-001	Jul-96	90.015	0.031	40.938	0.038	99.049	0.064	99.014	0.066
3718-001	Sep-96	90.009	0.015	41.042	0.020	99.222	0.035	99.194	0.036
3718-001	Oct-96	89.996	0.026	41.046	0.007	99.226	0.009	98.806	0.009
3718-001	Dec-96	89.981	0.020	41.038	0.035	99.210	0.061	99.172	0.063
3718-003	Jul-96	89.934	0.035	40.754	0.046	98.730	0.075	98.683	0.079
3718-003	Sep-96	89.964	0.013	40.879	0.010	98.941	0.017	98.907	0.017
3718-003	Oct-96	89.932	0.015	40.868	0.009	98.918	0.015	98.491	0.016
3718-003	Dec-96	89.929	0.029	40.872	0.063	98.925	0.107	98.879	0.113
3562-005	Jul-96	89.795	0.049	53.048	0.056	1008.125	0.039		
3562-005	Sep-96	89.853	0.034	53.202	0.113	1008.005	0.106		
3562-005	Oct-96	89.811	0.014	53.198	0.050	1007.991	0.041		
3562-005	Dec-96	89.826	0.074	53.230	0.146	1007.960	0.129		
3738-001	Jul-96	89.963	0.055	34.327	0.059	1035.740	0.175		
3738-001	Sep-96	89.990	0.045	34.448	0.073	1035.530	0.200		
3738-001	Oct-96	89.956	0.040	34.447	0.041	1035.478	0.123		
3738-001	Dec-96	89.983	0.023	34.406	0.031	1035.536	0.129		

NIST Technical Publications

Periodical

Journal of Research of the National Institute of Standards and Technology—Reports NIST research and development in those disciplines of the physical and engineering sciences in which the Institute is active. These include physics, chemistry, engineering, mathematics, and computer sciences. Papers cover a broad range of subjects, with major emphasis on measurement methodology and the basic technology underlying standardization. Also included from time to time are survey articles on topics closely related to the Institute's technical and scientific programs. Issued six times a year.

Nonperiodicals

Monographs—Major contributions to the technical literature on various subjects related to the Institute's scientific and technical activities.

Handbooks—Recommended codes of engineering and industrial practice (including safety codes) developed in cooperation with interested industries, professional organizations, and regulatory bodies.

Special Publications—Include proceedings of conferences sponsored by NIST, NIST annual reports, and other special publications appropriate to this grouping such as wall charts, pocket cards, and bibliographies.

National Standard Reference Data Series—Provides quantitative data on the physical and chemical properties of materials, compiled from the world's literature and critically evaluated. Developed under a worldwide program coordinated by NIST under the authority of the National Standard Data Act (Public Law 90-396). NOTE: The Journal of Physical and Chemical Reference Data (JPCRD) is published bimonthly for NIST by the American Chemical Society (ACS) and the American Institute of Physics (AIP). Subscriptions, reprints, and supplements are available from ACS, 1155 Sixteenth St., NW, Washington, DC 20056.

Building Science Series—Disseminates technical information developed at the Institute on building materials, components, systems, and whole structures. The series presents research results, test methods, and performance criteria related to the structural and environmental functions and the durability and safety characteristics of building elements and systems.

Technical Notes—Studies or reports which are complete in themselves but restrictive in their treatment of a subject. Analogous to monographs but not so comprehensive in scope or definitive in treatment of the subject area. Often serve as a vehicle for final reports of work performed at NIST under the sponsorship of other government agencies.

Voluntary Product Standards—Developed under procedures published by the Department of Commerce in Part 10, Title 15, of the Code of Federal Regulations. The standards establish nationally recognized requirements for products, and provide all concerned interests with a basis for common understanding of the characteristics of the products. NIST administers this program in support of the efforts of private-sector standardizing organizations.

Order the **following** *NIST publications—FIPS and NISTIRs—from the National Technical Information Service, Springfield, VA 22161.*

Federal Information Processing Standards Publications (FIPS PUB)—Publications in this series collectively constitute the Federal Information Processing Standards Register. The Register serves as the official source of information in the Federal Government regarding standards issued by NIST pursuant to the Federal Property and Administrative Services Act of 1949 as amended, Public Law 89-306 (79 Stat. 1127), and as implemented by Executive Order 11717 (38 FR 12315, dated May 11, 1973) and Part 6 of Title 15 CFR (Code of Federal Regulations).

NIST Interagency or Internal Reports (NISTIR)—The series includes interim or final reports on work performed by NIST for outside sponsors (both government and nongovernment). In general, initial distribution is handled by the sponsor; public distribution is handled by sales through the National Technical Information Service, Springfield, VA 22161, in hard copy, electronic media, or microfiche form. NISTIR's may also report results of NIST projects of transitory or limited interest, including those that will be published subsequently in more comprehensive form.

U.S. Department of Commerce
National Institute of Standards
and Technology
Gaithersburg, MD 20899–0001